ACTPAC

Funded by the European Union

ACTPAC	
Project number:	101135289
Project name:	A Complete Transformation PAth for C-C backboned plastic wastes to high-value Chemicals and materials
Topic:	HORIZON-CL6-2023-ZEROPOLLUTION-01-5
Type of action:	HORIZON-IA
Starting date of action:	01.01.2024
Project duration:	48 months
Project end date:	31.12.2027
Deliverable number:	D4.2
Deliverable title:	Successfully designed alkane converting bacterial strains for mid to long-chain diol production
Document version:	Ver2
WP number:	WP4
Lead beneficiary:	3 - UM
Main author(s):	Jochen Schmid (03-UM), Giulia Ravagnan (03-UM), Ann-Sophie Jochmann (03-UM)
Internal reviewers:	Bekir Engin Eser (01-AU)
Nature of deliverable:	R
Dissemination level:	PU
Delivery date from Annex 1:	30th June 2025
Actual delivery date:	30th June 2025

Funded by the European Union. Views and opinions expressed are however those of the author(s) only and do not necessarily reflect those of the European Union or REA. Neither the European Union nor the granting authority can be held responsible for them.

Document history

Version	Date	Beneficiary	Description
0.1	27.06.2025	03 - UM	For internal review
0.2	29.06.2025	03 - UM	Internally reviewed by Jochen Schmid
0.3	30.06.2025	03 - UM	Edited by Ann-Sophie Jochmann
0.4	30.06.2025	01 - AU	Internally reviewed by Bekir Engin Eser
1.0	30.06.2025	03 - UM	Finally reviewed by Giulia Ravagnan & Jochen Schmid

Executive Summary

α-ω-alkane diols and α-ω-alkane dicarboxylic acids are important building blocks for polyesters. For their production, biocatalytic methods are increasingly researched as alternatives to the traditional, chemical, multi-step, energy-intensive production processes [1–3]. To date, microbial α-ω-alkane to diol conversion has been focused on diols of short to mid-chain length up to C12, mainly by using the well-studied alkane hydroxylase AlkB from *Pseudomonas putida* GPo1 (*P. putida* GPo1) [3, 4] or CYP52s [5, 6] known to work up to C12 alkanes. Yet, α-ω-alkane diols of longer chain length are highly desirable since the chain length of the building blocks highly affects the properties of the resulting polyesters, such as flexibility and biodegradability. Next to the chain length, the substrate and product tolerance of the microorganisms that will be used for the conversion is of high importance to realize an economically feasible production process. *Pseudomonas* sp. and *Paenibacillus* sp. are known to be solvent-tolerant microorganisms that are also genetically accessible and, by that, can be efficiently engineered [7–9].

To evaluate if *Paenibacillus polymyxa* can be a potential alternative to the already described *Pseudomonas* strains and can be engineered towards diol production from long-chain alkanes, five plasmids were constructed and transferred to *P. polymyxa* DSM 365 to test long-chain α-ω-diol bioproduction. The first plasmid pHEiP_*alkBLGTS* contains all the genes necessary for alkane hydroxylation that naturally occur in the OCT plasmid of *P. putida* GPo1, serving as a control. For the plasmids pHEiP_alkB1LGTS and pHEiP_*alkB2LGTS*, the AlkB encoding gene from *P. putida* was exchanged with the AlkB1 and AlkB2 encoding genes from *R. erythropolis* PR4. These hydroxylases are known to hydroxylate C12 to C16 alkanes. In the plasmids pHEiP_akB1cluster+alkL and pHEiP_*alkB*2cluster+rub+*alkL*, the AlkB1 and AlkB2 encoding genes are present together with the rubredoxins, rubredoxin reductase, and transcriptional regulators that naturally occur in the *R. erythropolis* PR4 alkane degradation clusters. Different test cultivations of the variants equipped with the different constructs were carried out. But unfortunately, for none of the mutants, diol production by use of C12 alkane as substrate could be obtained. Based on that, an optimization strategy to address potential bottlenecks and evaluation of alternative strains was started.

Due to their well-documented robustness and metabolic versatility, two *Pseudomonas* strains were selected as alternative hosts: *Pseudomonas fluorescens* SBW25 and *P. putida* KT2440. To enable alkane conversion in these hosts, different plasmids were constructed by inserting *P. putida* GPO1 *alk* genes into the pWBT plasmid backbone for both strains and the pSEVA plasmid backbone for *P. putida* KT2440. The *alk* operon was also rearranged to identify and address putative rate-limiting steps and versions with an alternative T5 promoter were constructed to test possible expression limitations. By that the plasmids pWBT_*alkBLGST*, pWBT_*alkGBLST*, pWBT_*alkGFBLST*, pWBT_T5_alkBLGT and pWBT_T5_alkGBTL were constructed and transferred to *P. fluorescens*. Plasmids pWBT_*alkBLGST*, pWBT_*alkGBLST* and pWBT_*alkGFBLST* were also transferred into *P. putida* KT2440. Additionally, pSEVA258_*alkB*FLG*T* was heterologously expressed in *P. putida* KT2440. This plasmid carries the Pm promoter under the control of XylS to regulate the expression of the *alk* gene. In addition, the *alkB* and *alkG gene* sequences are modified to minimize the effect of carbon catabolite repression on the system. All variants were tested for growth on alkanes as sole substrate as well as conversion towards diols. As a control, if short or mid- to long-chain alkanes are accepted, hexane (C6) was also tested. In

addition, several cultivation conditions were analysed. By that approach, *P. fluorescens* carrying pWBT_*alkGFBLST* was enabled to grow on alkanes for the first time. For *P. putida* KT2440 pWBT_*alkGFBLTS* and *P. putida* KT2440 pSEVA258_*alkB*FLG*T* the production of hexanol and hexanoic acid from hexane was realized for the first time. From *P. putida* KT2440 pWBT_*alkGFBLST* 0.77 mM hexanol and 0.76 mM hexanoic acid were obtained. For *P. putida* KT2440 pSEVA258_*alkB*FLG*T* 0.70 mM hexanol and 0.67 mM hexanoic acid were obtained. No production of diols was observed in the small-scale conversions, and an overoxidation (hexanoic acid) was observed. These results demonstrate the functionality of the chosen approach for alkane oxidation and provide a strong foundation for further engineering toward efficient long-chain diol production. The issues of overoxidation and only one alcohol group at the alkanes will be addressed by further gene knock outs and engineering approaches.

Finally, docking studies and molecular dynamics simulations were performed to further understand the AlkB system in use and explore new future solutions. For this esterification was identified as a promising solution.

If these mentioned approaches will not work out the bacterial long chain alkane to diol conversion must be evaluated critically for the ACTPAC project. But finally, several highly valuable and promising insights were obtained for the project within D4.2 to complete WP4.

Content

Executive Summary 1
List of Figures 4
List of Tables 6
Acronyms & Abbreviations 6
1 Introduction 7
1.1 Overview 7
1.2 Relation to other Tasks and Deliverables 10
1.3 Structure of the Deliverable 10
2 Main section 11
2.1 *Paenibacillus polymyxa* DSM 365 11
2.1.1 Testing Tolerance of *P. polymyxa* DSM 365 against dodecane 11
2.1.2 Research on C12 to C16 Converting AlkB like Alkane Hydroxylases 11
2.1.3 Plasmid Design and Strain Engineering for Alkane based α-ω-Diol Conversion in *P. polymyxa* DSM 365 13
2.1.4 Test Cultivations using Mutant *P. polymyxa* DSM 365 Strains for Dodecane to 1,12-Dodecanediol conversion 16
2.2 *Pseudomonas fluorescens* 18
2.2.1 Assessing the Presence of Alkane Degradation Genes in Candidate Strains Through BLAST analysis 18
2.2.2 Assessing Growth on Alkanes of *P. fluorescens* SBW25 on Solid Media 19
2.2.3 Genetic Engineering of *P. fluorescens* SBW25 19
2.3 *Pseudomonas putida* KT2440 25
2.3.1 Plasmid Design and Strain Engineering for Alkane to α-ω-Diol Conversion in *P. putida* KT2440 25
2.3.2 Test Cultivations Using Mutant *P. putida* KT2440 Strains for Alkane Oxidation 27
2.4 In Silico Analysis of AlkB Reaction System 28
2.4.1 Docking Studies of AlkB 28
2.4.1 Substrate Behaviour in Membrane 29
2.4.2 Alkane Movement in Membrane 30
2.4.3 Alcohols and Esters Movement in Membrane 32
3 Conclusions 34
4 References 36

List of Figures

Figure 1: Pathway of alkane degradation in *P. putida* GPO1. AlkL transports alkanes across the outer membrane. AlkT oxidises NADH and transfers electrons to AlkG which transfers them onto the membrane bound alkane hydroxylase AlkB. An alcohol dehydrogenase (AlkJ) and aldehyde dehydrogenase (AlkH) convert fatty alcohols to fatty acids, which are then transformed by AlkK to acyl-CoA. Both clusters are induced by AlkS. The transcription of *alkS* is activated in the presence of alkanes or DCPK [15]. 8

Figure 2: Alkane to α,ω-diol conversion using AlkBGT from *P. putida* (adapted from [17]) 9

Figure 3: Growth of *P. polymyxa* DSM 365 with different dodecane concentrations. Cultures were grown in 25 mL MOPPA minimal media in 250 mL shake flasks at 30 °C and 200 rpm. Dots indicate the mean, error bars the standard deviation (n = 2). 11

Figure 4: pHEiP_*alkBLGST*, containing the pHEiP backbone including a neomycin resistance gene for selection, *alkB* encoding the alkane hydroxylase, *alkG* and *alkT* encoding the rubredoxin and rubredoxin reductase from, *alkL* encoding the alkane transporter and *alkS*. 14

Figure 5: Organisation of the *alkB1* and *alkB2* cluster in *R. erythropolis* PR4. *alkB1* and *alkB2* are encoding the respective hydroxylase, *rubA1-rubA4* are encoding rubredoxins, *rubB* encodes a rubredoxin reductase and *alkU1* and *alkU2* are encoding putative TetR family transcriptional regulators (adapted from [21]) 15

Figure 6: Schematic drawings of the plasmid constructs pHEip_*alkB1LGST*, pHEiP_*alkB2LGST*, pHEiP_*alkB1*cluster+*alkL* and pHEiP_*alkB2*cluster+*rub*+*alkL*. Genes derived from *P. putida* GPo1 are marked in purple. Genes derived from *R. erythropolis* PR4 *alkB1* cluster are marked in dark green. Genes derived from *R. erythropolis* PR4 *alkB2* cluster are marked in yellow. 15

Figure 7. Growth of *P. fluorescens* SBW25 and *P. aeruginosa* PAO1 on M9 agar plates containing no carbon source. 500 µL of alkanes were either applied directly onto plate (top plates) or supplied through gas phase (bottom plates). Cells were grown for 5 days at 30°C. P. fluorescens shows some limited growth which can be attributed to organic contaminants in the used agar, as this growth was also present on plates with no alkanes. 19

Figure 8. pWBT_Palk_*alkBLGST* plasmid. Plasmid constructed from the pWBT plasmid via the exchange of the T5 lac promoter. The two operons *alkST* and *alkBLG* of *P. putida* GPO1 are arranged under their native promoters. 20

Figure 9. *P. fluorescens* pWBT_Palk_*alkBLGST* on M9 agar plates with only dodecane as carbon source. On the left, the control without dodecane (no C-source), on the right, the strain with supplied dodecane. The strain was incubated for 4 days at 30 °C. 21

Figure 10. Growth of *P. fluorescens* SBW25 on M9 plates without additional carbon source with either plasmids pWBT_Palk_*alkBLGST*, pWBT_Palk_*alkGBLST*, pWBT_T5_*alkBLGT,* or pWBT_T5_*alkGBTL*. Dodecane was supplied through the gas phase to the upper plates, with the lower plates being the negative control. 22

Figure 11: Growth of *P. fluorescens* SBW25 in M9 medium with either pWBT_Palk_*alkGBLST* or pWBT_T5_*alkBLGT*, with or without dodecane as C-source. Cells were grown to OD_{600} of 0.5 before being induced with either 0.05 % DCPK for Palk or 1 mM IPTG for PT5. Cells were grown at 30°C at 120 rpm. Dots indicate the mean, error bars the standard deviation (n = 2)..... 22

Figure 12. Growth of *P. fluorescens* SBW25 in M9 medium with 2 g/L citrate using different construct variations: base refers to pWBT_Palk_*alkGBLST* without *alkF*. The *alkF* constructs refer to the strain variants with pWBT_Palk_*alkGFBLST* that includes *alkF*. Cells were grown at 30 °C at 120 rpm with 0.05 % of DCPK added from the beginning. Negative controls did not contain any alkanes, while the other cultures contained 1 % dodecane from the beginning on, with additional 1 % dosage after 3 days. Dots indicate the mean, error bars the standard deviation (n = 2)..... 23

Figure 13. Growth of *P. fluorescens* SBW25 in M9 medium with 2 g/L citrate using different construct variations: base refers to pWBT_Palk_*alkGBLST* without *alkF*. The *alkF* refers to the strain with pWBT_Palk_*alkGFBLST* that includes *alkF*. Cells were grown at 30 °C at 120 rpm with 0.05 % of DCPK added from the beginning on. Negative controls did not contain any alkanes, while the other cultures contained 1 % dodecane from the beginning on with another dosage of 1 % after 3 days. The wildtype without alkanes aggregated quite strongly, causing a stronger decrease in OD_{600}. Squares indicate the mean, error bars the standard deviation (n = 2)..... 24

Figure 14: Schematic structure of pSEVA_*alkB*FLG*T* including a neomycin resistance gene for selection and *XylS* for induced activation of the Pm promoter, *alkB** encoding a modified version of the alkane hydroxylase from the OCT plasmid, modified *alkG* and *alkT* encoding the rubredoxin and rubredoxin reductase from the OCT plasmid, *alkL* encoding the alkane transporter from the OCT plasmid. 26

Figure 15: Chromatogram from the first replica (n1) of from the conversion with *P. putida* KT2440 pWBT *alkGFBLTS.* 27

Figure 16: Obtained titers of hexanol and hexanoic acid from the conversions using *P. putida* KT2440 pWBT_a*lkGFBLST* and *P. putida* KT2400 pSEVA258_*alkB*FLG*T*. Columns indicate the mean, error bars the standard deviation (n =2)..... 28

Figure 17. [A] Snapshot of a molecular dynamics simulation run shows dodecane leaving the P. fluorescens SBW25 AlkB substrate channel into the membrane. [B] Density plot of the membrane and AlkB after a 50 ns run. The membrane shows its highest density around the head groups, with the density decreasing towards the mobile lipid tails..... 29

Figure 18. Example of the methodology for tracking molecule movement in the membrane along the z axis shown for the C1 atoms of five dodecane over 25 ns. Index groups of the terminal heavy atoms were created and tracked over the run as well as the membrane COM. The positions were then normalized against the membrane center of mass and the fraction of time spend within 0.6 nm determined..... 30

Figure 19. Exemplary positions of dodecane during a simulation run. Shown in opaque are the dodecane molecules with the membrane lipids displayed see-through and the water molecules hidden. 31

Figure 20. Histogram of the distance of the terminal carbon atoms of dodecane to the membrane COM over a 200 ns run. Only one terminal atom per molecule was tracked for this graph. 31

Figure 21. Exemplary positions of dodecanol during a run. Shown in opaque are the dodecane molecules with the membrane lipids displayed see-through and the water molecules hidden. 32

Figure 22. Extrapolated fraction of different compounds with both molecules ends within 0.6 nm of the membrane center. Five molecules of each substrate were inserted into a membrane system, and the simulation ran for 200 ns. Shown from left to right are alkanes, alcohols, and esters, with the chain length of both chains of the ester given (n = 1). 33

List of Tables

Table 1: D4.2 Output for other tasks and deliverables. 10

Table 2: Alkane monooxygenases hydroxylating alkanes of a chain length of C12 to C18 as considered for ACTPAC. 12

Table 3: Mutant *P. polymyxa* DSM 365 strains readily prepared for alkane to α-ω-diol conversion. . 16

Table 4: Summarized cultivation and extraction methods for dodecane to 1,12-dodecanediol conversion by use of the different created mutants of *P. polymyxa* DSM 365. 17

Table 5: BlastP results for the *P. putida* GPO1 proteins for alkane hydroxylation and the proteins of *P. fluorescens* SBW25. 18

Table 6: Mutant variants of *P. fluorescens* SBW25 engineered for alkane to α-ω-diol conversion..... 24

Table 7: Mutant *P. putida* KT2440 strains constructed for alkane to α-ω-diol conversion. 26

Acronyms & Abbreviations

Term	Description
P. putida	*Pseudomonas putida*
Crc	Catabolite Repression Control
CYP	Cytochrom P450
DCPK	Dicyclopropylketon
E. coli	*Escherichia coli*
Hfq	Host factor for Qβ replicase
MD	Molecular Dynamics
OD_{600}	Optical Density at 600 nm
P. polymyxa	*Paenibacillus polymyxa*
R. erythropolis	*Rhodococcus erythropolis*

1 Introduction

1.1 Overview

The scope of this deliverable is to design bacterial strains for the conversion of n-alkanes to α-ω-alkane diols of a chain length between C12 and C18.

Traditionally, α-ω-alkane diols are produced via chemical-synthetic processes. In these processes, high temperatures and pressures must be applied to enable hydroxylation of alkanes, rendering them highly energy demanding and thus not sustainable. These processes also depend on the use of metal-catalysts with a high environmental toxicity. Additionally, the low regioselectivity of these reactions results in the formation of numerous side products, reducing overall efficiency and increasing environmental pollution [10, 11] .

Using microbial whole-cell catalysts for the conversion of n-alkanes to α-ω-alkane diols is a promising option to make diol production more sustainable [1]. The enzymatic biocatalysts involved in the hydroxylation of alkanes, can work at moderate temperatures and pressures, while providing a high regioselectivity [1, 6]. Furthermore, the biocatalysts as well as the microbial cells containing them are biodegradable, by that avoiding the outcome of environmental toxic wastes in such processes [12].

In nature, different enzymes can perform terminal hydroxylation of alkanes. Important enzyme groups supporting the desired reaction on alkanes of a chain length from C12 to C18 under aerobic conditions are AlkB-like monooxygenases, prokaryotic cytochrome P450 monooxygenases (CYP153 family), and eukaryotic cytochrome P450 monooxygenases (CYP52 family). All three types are naturally involved in n-alkane consumption for growth. The products of the hydroxylation as performed by these enzymes are 1-alkanols. In the native microbial systems these 1-alkanols then undergo further oxidations and finally enter the β-oxidation pathway, where they are fully degraded for energy production [13, 14].

A well-studied alkane degradation system origins from *P. putida* GPo1 which naturally carries the OCT plasmid. This plasmid encodes for nine genes which are involved in alkane degradation, organised in two gene clusters. The first cluster *alkBFGHJKL* encodes all proteins for the hydroxylation of alkanes and oxidation of the alcohols to fatty acids except AlkT, which is encoded in the second cluster *alkST*. The second cluster also encodes for AlkS, the transcriptional regulator of both clusters. When alkanes enter the cell, AlkS activates transcription [15].

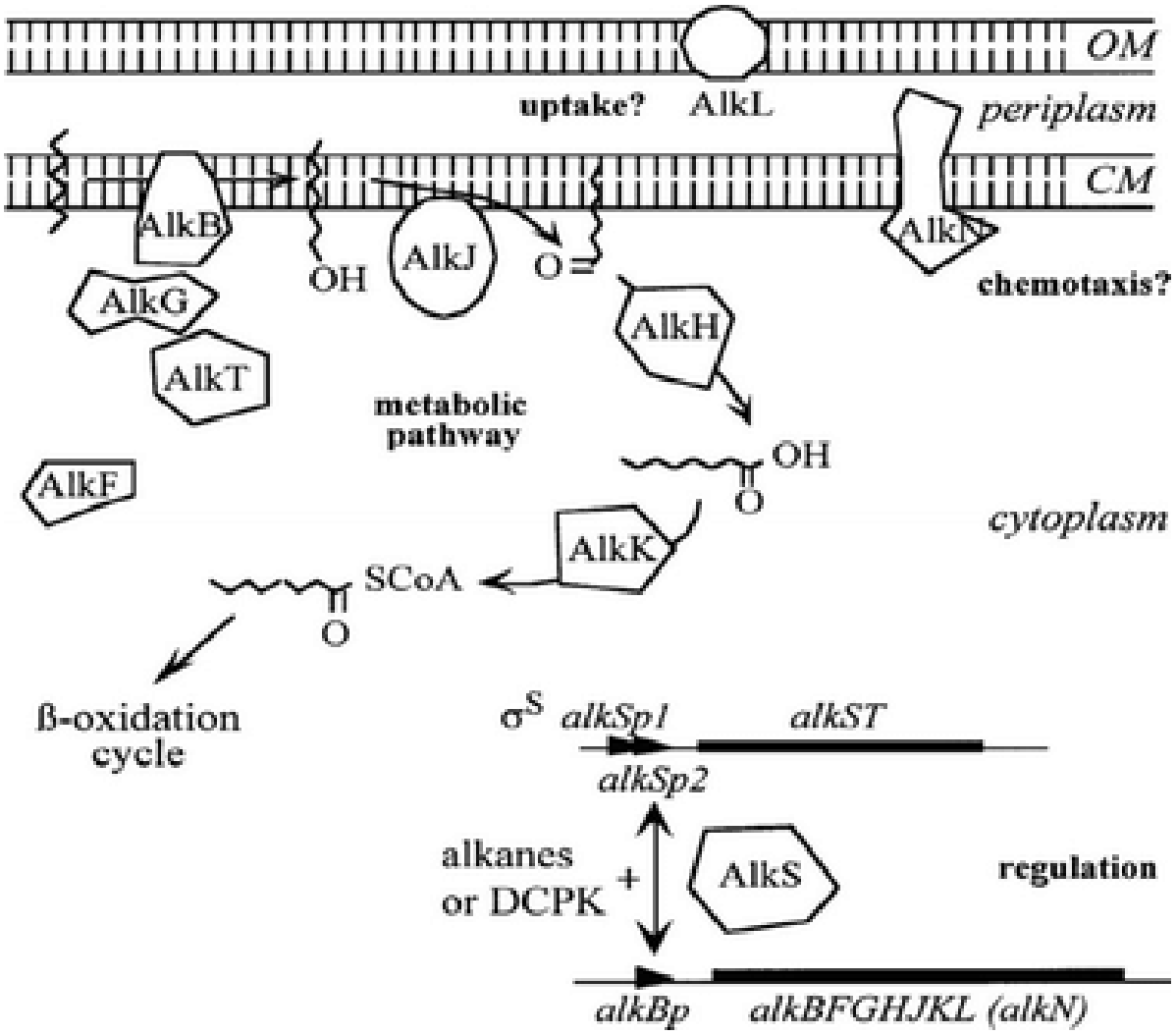

Figure 1: Pathway of alkane degradation in *P. putida* GPO1. AlkL transports alkanes across the outer membrane. AlkT oxidises NADH and transfers electrons to AlkG which transfers them onto the membrane bound alkane hydroxylase AlkB. An alcohol dehydrogenase (AlkJ) and aldehyde dehydrogenase (AlkH) convert fatty alcohols to fatty acids, which are then transformed by AlkK to acyl-CoA. Both clusters are induced by AlkS. The transcription of *alkS* is activated in the presence of alkanes or DCPK [15].

A valid strategy to use the hydroxylases for efficient diol formation, is the plasmid born expression of the hydroxylase encoding genes in parallel with genes supporting the reaction (e.g., for electron transport) in a non-alkane-degrading organism. This will avoid further oxidation after the hydroxylation and allow product accumulation [1, 3, 5, 6, 16]. Whilst 1-alkanols remain the predominant products from those attempts, the formation of diols was also demonstrated [6].

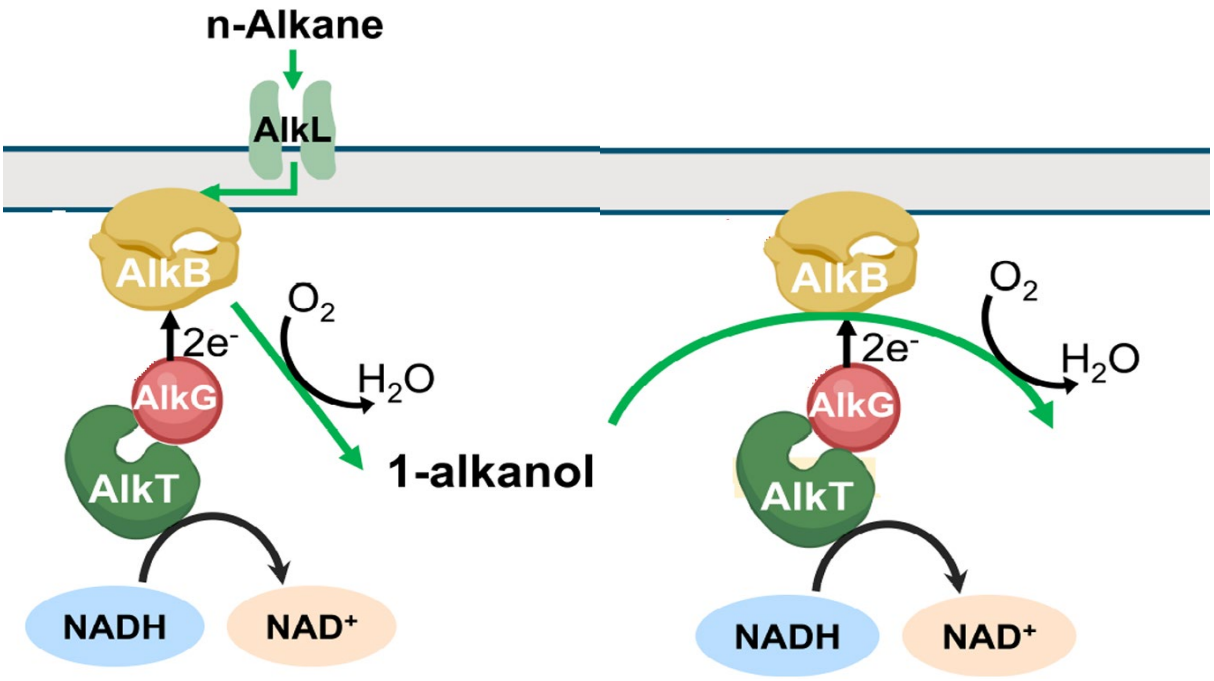

Figure 2: Alkane to α,ω-diol conversion using AlkBGT from *P. putida* (adapted from [17])

Using the alkane hydroxylase AlkB from *P. putida* together with its supporting rubredoxin AlkG and rubredoxin reductase AlkT under the regulation of their natural promoter and the activator AlkS in combination with the Atf1 acetyltransferase in *E. coli* has led to the highest reported titer in microbial diol precursor production of 9.20 mM 1,6-diacetoxyhexane and 2.23 mM 6-hydroxy hexyl acetate so far [4]. Therefore, this system seems to be a promising base to develop an efficient process for diol production using microbes as whole-cell biocatalysts.

But, the substrate specificity of AlkB from *P. putida,* ranging from C5 to C12 [18], does not cover the whole range of alkanes as targeted in the ACTPAC project. For this, the system must be modified Towards the acceptance of C12 to C18 alkanes. A logical approach is the use of alkane hydroxylases with a suitable substrate range, in their natural genetic environment or in the combination with the enzymes from the OCT plasmid. Putative hydroxylase candidates can derive from different genera such as *Rhodococcus, Acinetobacter,* or *Mycobacterium* [19–21].

Next to suitable enzymes, the selection of the most promising production host is crucial for an efficient bioprocess. Important characteristics include growth rate, tolerance against substrate and product as well as handling, of the complete bioprocess [22, 23].

P. polymyxa DSM 365 is a Gram-positive, spore-forming bacterium naturally occurring in the rhizosphere of plants [24], which is known to produce more than 100 g/L of the organic solvent 2,3-butanediol [8], highlighting it's robustness against organic solvents and rendering it a promising candidate for the production of diols in general. In addition, various highly efficient genetic and genomic engineering tools are established and latest progress in the development of genome-reduced mutants of that strain offer high potential for the use as an efficient microbial cell factory [9].

Apart from *P. polymyxa* also *Pseudomonas* has been discussed in recent years as a promising production organism for α-ω-alkane derived diol production [17]. The alkane to α-ω-alkane diol precursor conversion has been demonstrated successfully by use of that host [1, 2]. Several

Pseudomonas sp. strains have been shown to endure harsh cultivation conditions for example, in the presence of different organic acids [25] and solvents as phenol [7]. In addition, they provide a versatile metabolism with a high capacity to perform difficult redox reactions, and genetic modification tools are well established, making it another promising candidate for α-ω-diol production [26].

In general, the mechanism of the uptake, transport, and distribution within the outer membrane of Gram-negative bacteria is not elucidated yet and remains elusive up to now. The same is true for Gram-positive bacteria, which have only an inner membrane in combination with a much thicker murein sacculus. To analyse the mechanism of AlkB, which has been widely used for alkane hydroxylation, a thorough study using docking and molecular dynamics simulations was performed. This approach was intended to give further insights into substrate distribution and availability to AlkB.

1.2 Relation to other Tasks and Deliverables

This deliverable is related to the following other ACTPAC tasks and deliverables:

Receives inputs from:

This deliverable does not receive inputs from another deliverable.

Provides outputs to:

Table 1: D4.2 Output for other tasks and deliverables.

Deliverable	Due Date	Output from D4.2
D5.1	32	D4.2 delivers first functional bacterial strains for alkane to α-ω-diol conversion to deliverable 5.1, so that they can be used for the development of efficient bioprocesses.
D5.2	36	D4.2 delivers first functional bacterial strains for alkane to α-ω-diol conversion to deliverable 5.2, so that they can then be further optimised.
D10.5	36	D4.2 delivers first functional bacterial strains for alkane to α-ω-diol conversion to deliverable 10.5, so that they can be used for the development of efficient 20 L bioprocesses and demonstration of production at 100/100 L scale.
D10.6	36	D4.2 delivers first functional bacterial strains for alkane to α-ω-diol conversion, so that an upscale process can be developed and then reported in deliverable D10.6.

1.3 Structure of the Deliverable

In this deliverable, our results are presented in chapter 2. We present the results divided into three subsections according to the three strains that were engineered. Afterwards, a combined conclusion of the work for this deliverable is presented in chapter 3.

2 Main section

2.1 *Paenibacillus polymyxa* DSM 365

2.1.1 Testing Tolerance of *P. polymyxa* DSM 365 against dodecane

To check the suitability of *P. polymyxa* DSM 365 for the aspired process to accept high concentrations of mid- to long-chain alkanes as substrate, we performed cultivations in the presence of different amounts of dodecane as a model substrate. By the obtained results, no correlation of the dodecane concentration and the reached biomass (OD_{600}) was observed. Even for the highest dodecane concentration of 50 g/L the growth was not significantly affected compared to the control with 0 g/L of dodecane. Therefore, it was concluded that the tolerance of *P. polymyxa* against mid- to long-chain alkanes is sufficient for the purposes of ACTPAC and that this organism is a suitable candidate for the targeted bioprocess.

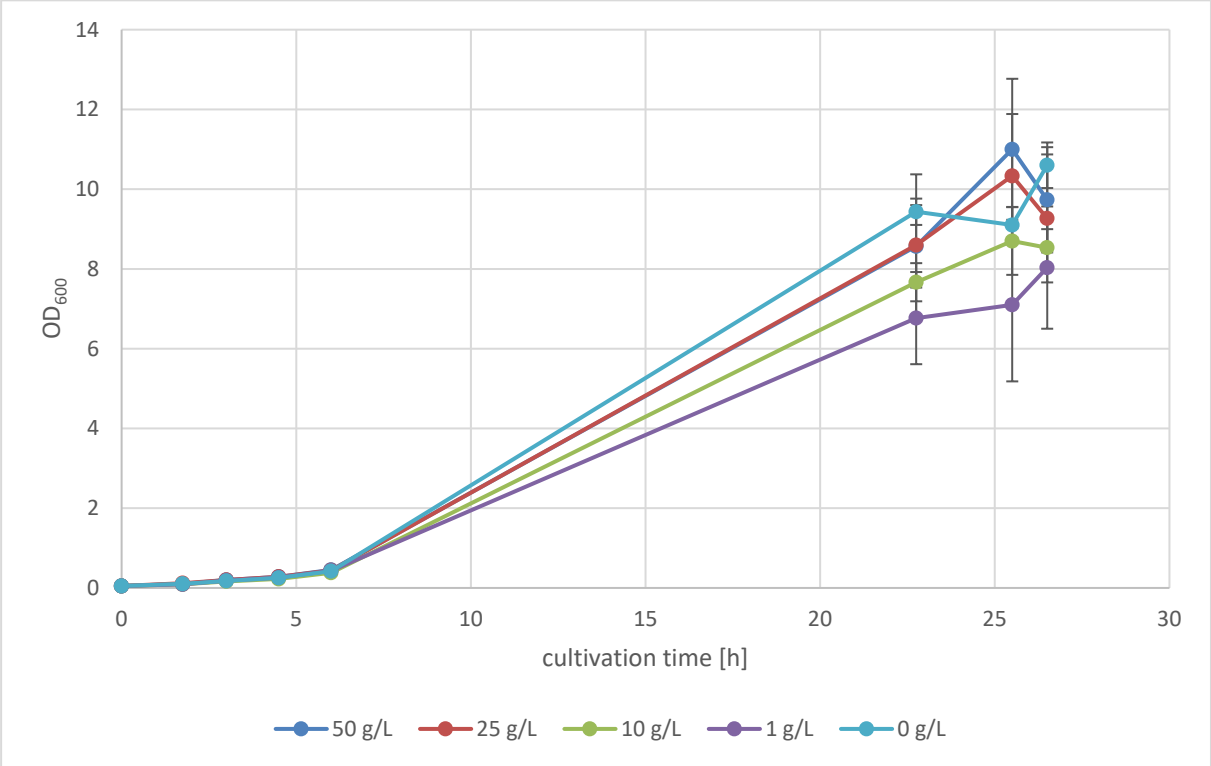

Figure 3: Growth of *P. polymyxa* DSM 365 with different dodecane concentrations. Cultures were grown in 25 mL MOPPA minimal media in 250 mL shake flasks at 30 °C and 200 rpm. Dots indicate the mean, error bars the standard deviation (n = 3).

2.1.2 Research on C12 to C16 Converting AlkB like Alkane Hydroxylases

As mentioned before, all published reports on diol production from alkanes by the use of whole cell biocatalysts are based on enzymes with a substrate specificity of C5 to C12 alkanes [18]. Since the aim of WP4 is the di-terminal hydroxylation of C12 to C18 alkanes, the enzymes used in these studies are not suitable for our purposes in their natural constitution. Therefore, a comprehensive literature research for suitable alternatives was conducted. Based on the fact that the highest titers for α-ω-diol

precursor production were achieved with AlkB from *P. putida* GPO1, we focused on AlkB-like monooxygenases. A list of all considered candidates is given in Table 2.

Table 2: Alkane monooxygenases hydroxylating alkanes of a chain length of C12 to C18 as considered for ACTPAC.

Enzyme	Origin	Risk classification [27]	Reported Substrate range/expression activation	Reported heterologous expression	Reference
AlkB	*Actinobacterium Gordonia* sp. strain SoCg	1	C12-C36	Yes	[28]
AlkM	*Acinetobacter* sp. ADP1	1	C12-C16	Not found	[19]
AlkM	*Acinetobacter calcoaceticus* EB104	2	C7-C18	Yes	[29] [30]
AlkMb	*Acinetobacter* sp. M-1	1	C16-C22	Yes	[31]
AlkB2	*Alcanivorax borkumensis* AP1	1	C10-C16	Yes	[32]
AlkB	*Burkholderia cepacian* RR10	2	C 10-C30	Not found	[30, 33]
AlkB	*Pseudomonas fluorescens* CHA0	1	C 12-C16	Yes	[20]
AlkB1	*Pseudomonas aeruginosa* PAO1	2	C12-C16	Yes	
AlkB2	*Pseudomonas aeruginosa* PAO1	2	C12-C16	Yes	[20]
AlkB2	*Pseudomonas aeruginosa* strain NY3	2	C12-C18	Not found	[34]
AlkB	*Mycobacterium tuberculosis* H37Rv	3	C11-C16	Yes	[20]

AlkB	*Prauserella rugosa* NRRL B-2295	1	C10-C16	Yes	[20]
AlkB2	*Rhodococcus erythropolis* Q15	1	C10-C16	Yes	[21]
AlkB2	*Rhodococcus erythropolis* NRRL B-16531	1	C10-C16	Yes	[21]
AlkB1	*Rhodococcus erythropolis* PR4	1	High upregulation at C16	No	[35]
AlkB2	*Rhodococcus erythropolis* PR4	1	Upregulation at C16	No	[35]

Due to the overall aim of the WP (non-pathogenic production host), all risk class 2 or 3 microorganisms were excluded from further considerations as production hosts, and also their genes were initially ranked second to avoid issues on safe utilization. Also, we decided against the AlkB monooxygenase from *Actinobacterium Gordonia* sp. strain and *Acinetobacter* sp. M-1 since the substrate specificity of the remaining candidates was more suitable in the natural structure of the enzymes. This decision was based on anticipating that fewer enzyme engineering efforts would be necessary, when it comes to narrowing down substrate specificity be. By that, the use of the *alkB1* and *alkB2* gene of *R. erythropolis* PR4 as promising candidates for encoding long chain alkane accepting proteins was decided. These enzymes show very high similarities to AlkB1 and AlkB2 from *R. erythropolis* Q15 (99.49 % identity for AlkB1 and 98.53 % for AlkB2 obtained in Blast comparison of amino acid sequences) and *R. erythropolis* NRRL B-16531 (99.74 % identity for AlkB1 and 99.26 % for AlkB2 obtained in Blast comparison of amino acid sequence). The AlkB2 monooxygenase of both strains has been expressed as a functional unit with other enzymes from the OCT plasmid in *E. coli* as well as in *P. putida* before. The same behaviour is therefore likely for the AlkB2 enzyme from *R. erythropolis* PR4, making it a promising candidate for our approach. In addition, highly detailed data are available on the upregulation of genes in *R. erythropolis* PR4 in the presence of hexadecane [15]. These findings offer valuable insights into the strain's alkane metabolism and played a key role in the decision to focus on the genes of this well-characterized organism. Though AlkB1 of *R. erythropolis* Q15 and *R. erythropolis* NRRL B-16531 were not functional in former tests when expressed together with the alkane degradation cluster from *P. putida* GPo1, we still wanted to keep AlkB1 from *R. erythropolis* PR4 as a candidate, since transcription data from *R. erythropolis* PR4 shows that it is highly expressed and upregulated in the presence of hexadecane [15].

2.1.3 Plasmid Design and Strain Engineering for Alkane based α-ω-Diol Conversion in *P. polymyxa* DSM 365

The pHEiP plasmid is an efficient molecular biological tool which was specifically designed for heterologous expression in *P. polymyxa* [36]. Therefore, it was chosen as the backbone for all constructs which were transferred into this strain. Firstly, the plasmid pHEiP_*alkBGTLS* was constructed, containing all the genes necessary for alkane hydroxylation, derived from the OCT plasmid

of *P. putida* GPo1 (Figure 4). The aim was to introduce set of genes that was successfully used for α-ω-diol production to our host of choice.

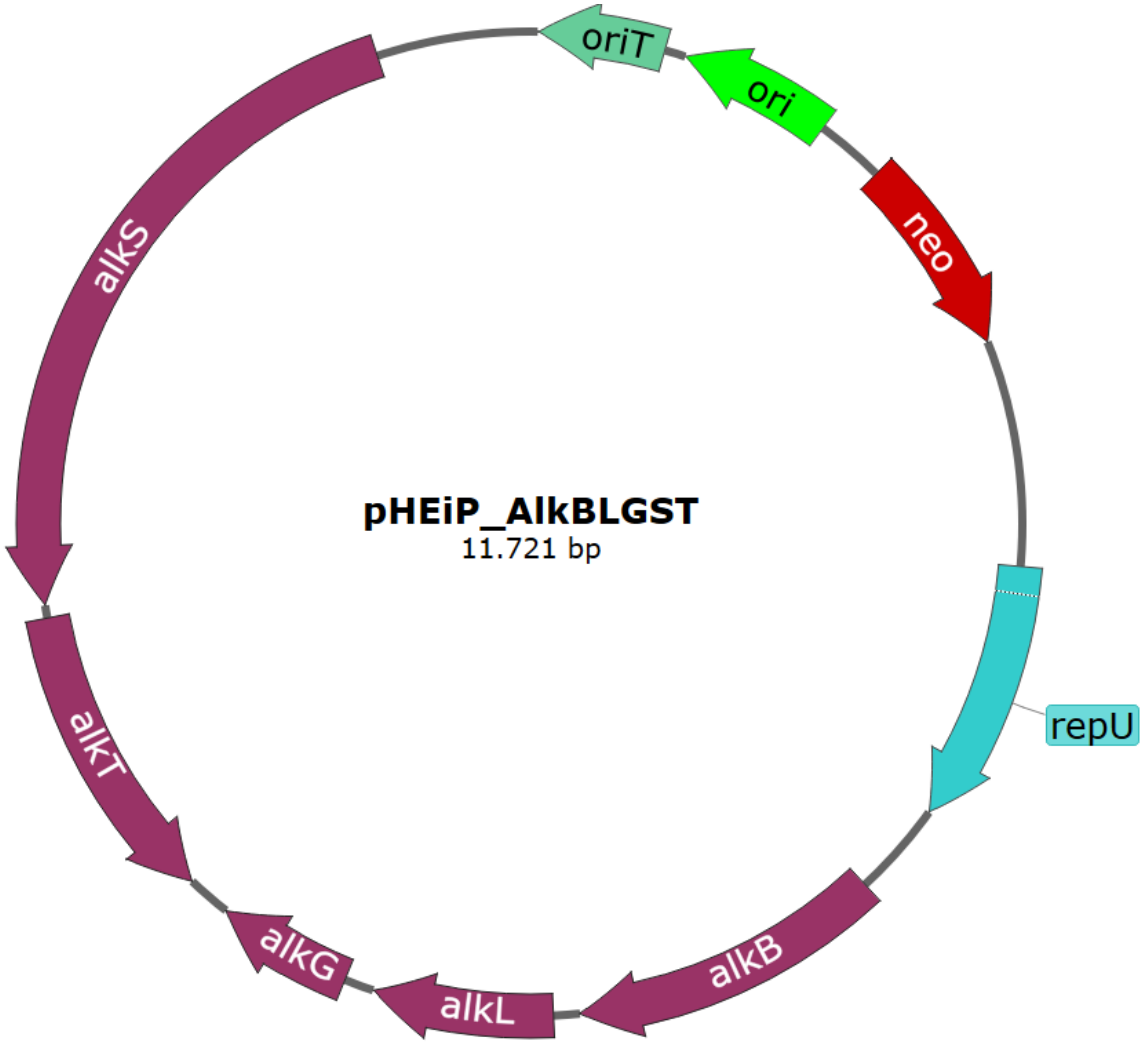

Figure 4: pHEiP_*alkBLGST*, containing the pHEiP backbone including a neomycin resistance gene for selection, *alkB* encoding the alkane hydroxylase, *alkG* and *alkT* encoding the rubredoxin and rubredoxin reductase from, *alkL* encoding the alkane transporter and *alkS*.

Based on the literature research on suitable AlkB hydroxylases, four more plasmids were designed for alkane hydroxylation in *P. polymyxa* DSM 365. The pHEiP_*alkB1LGST* and pHEiP_*alkB2LGST* constructs are derivates of the formerly designed pHEiP_*alkBLGST* (Table 3). In these plasmids, only the *alkB* gene was exchanged with the *alkB1* and *alkB2* genes from *R. erythropolis* PR4 respectively, to achieve conversion of the long-chain alkanes. Furthermore, the plasmids pHEiP_*alkB1*cluster+*alkL* and pHEiP_*alkB*2cluster+*rubB*+*alkL* were cloned, which contain the complete native gene clusters of which *alkB1* and *alkB2* were selected (Table 3). In the pHEiP_*alkB*2cluster+*rubB*+*alkL* construct, the *rubB gene* from the AlkB1 cluster was added, since it naturally does not contain a rubredoxin reductase [37].

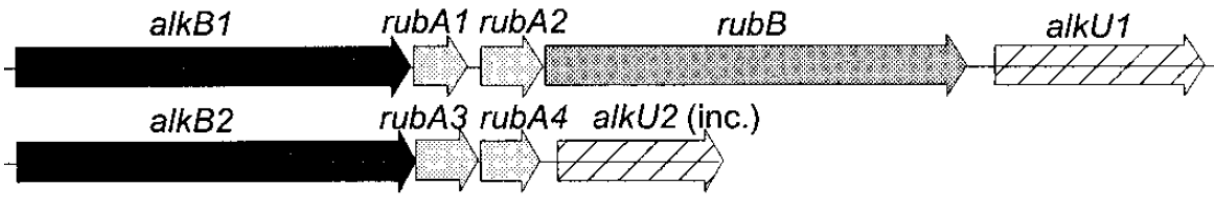

Figure 5: Organisation of the *alkB1* and *alkB2* cluster in *R. erythropolis* PR4. *alkB1* and *alkB2* are encoding the respective hydroxylase, *rubA1-rubA4* are encoding rubredoxins, *rubB* encodes a rubredoxin reductase and *alkU1* and *alkU2* are encoding putative TetR family transcriptional regulators (adapted from [21]) .

Finally, the *alkL* gene was added to both clusters since no alkane transporter is described for the Gram-positive *R. erythropolis* PR4. Schematic drawings of the plasmid maps for all constructs are given in Figure 6.

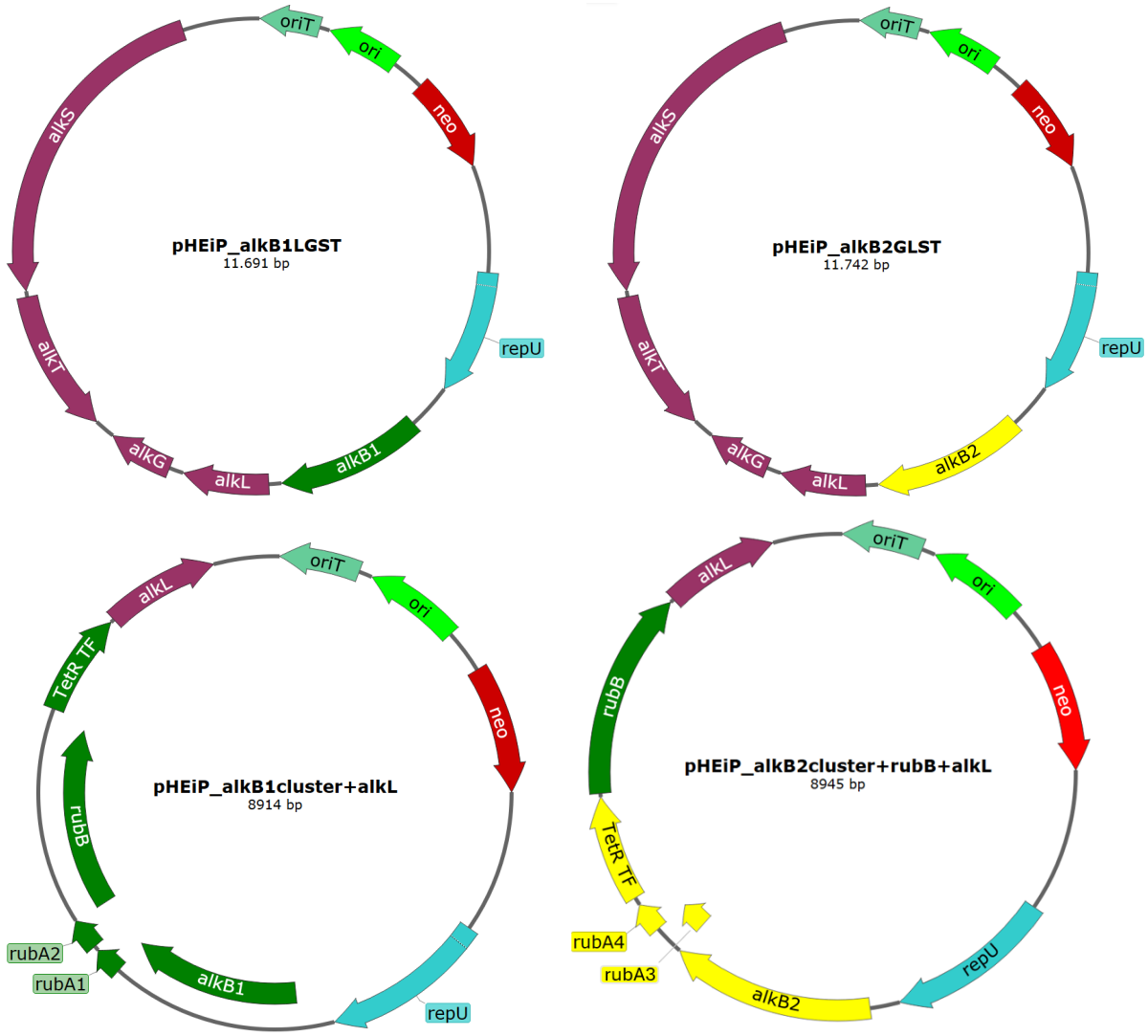

Figure 6: Schematic drawings of the plasmid constructs pHEip_*alkB1LGST*, pHEiP_*alkB2LGST*, pHEiP_*alkB1*cluster+*alkL* and pHEiP_*alkB2*cluster+*rub*+*alkL*. Genes derived from *P. putida* GPo1 are marked in purple. Genes derived from *R. erythropolis* PR4 *alkB1* cluster are marked in dark green. Genes derived from *R. erythropolis* PR4 *alkB2* cluster are marked in yellow.

All designed plasmids were successfully transferred to *P. polymyxa* DSM 365 via conjugation, resulting in five mutant strains (Table 3).

Table 3: Mutant *P. polymyxa* DSM 365 strains readily prepared for alkane to α-ω-diol conversion.

Strain	Plasmid	Description
P. polymyxa DSM 365 pHEiP_*alkBLGST*	pHEiP_*alkBLGST*	pHEiP equipped with all genes from *P. putida* GPo1 for terminal alkane hydroxylation
P. polymyxa DSM 365 pHEiP_*alkB1LGST*	pHEiP_*alkB1LGST*	pHEiP equipped with all genes for terminal alkane hydroxylation from *P. putida* GPo1, except *alkB* which was exchanged with *alkB1* from *R. erythropolis* PR4
P. polymyxa DSM 365 pHEiP_*alkB2LGST*	pHEiP_*alkB2LGST*	pHEiP equipped with all genes for terminal alkane hydroxylation from *P. putida* GPo1 exempt *alkB* which was exchanged with *alkB2* from *R. erythropolis* PR4
P. polymyxa DSM 365 pHEiP_*alkB*1cluster+*alkL*	pHEiP_*alkB*1cluster+*alkL*	pHEiP equipped with all genes for terminal alkane hydroxylation from the *alkB1* cluster from *R. erythropolis* and *alkL* from *P. putida* GPo1
P. polymyxa DSM 365 pHEiP_a*lkB2*cluster+*rub*+*alkL*	pHEiP_*alkB*2cluster+*rub*+*alkL*	pHEiP equipped with all genes for terminal alkane hydroxylation from the *alkB2* cluster from *R. erythropolis, rub* from the *alkB1* cluster from *R. erythropolis* and *alkL* from *P. putida* GPo1

2.1.4 Test Cultivations using Mutant *P. polymyxa* DSM 365 Strains for Dodecane to 1,12-Dodecanediol conversion

Multiple cultivation experiments for all mutants of *P. polymyxa* DSM 365 were performed to analyse their dodecane conversion ability. Batch cultivation as well as two step cultivations as reported in literature were performed [3, 4]. In addition, cultivations with and without TWEEN 80 as an emulsifier, to tune the substrate accessibility were performed. For product analysis, cell disruption with an ultrasonic treatment was applied to analyse product extraction from this solvent tolerant, Gram-positive organism. Main characteristics of the different setups are listed in Table 4. Finally, for all the multiple setups which have been tested, the targeted alkane hydroxylation could not be proven by analysis of the supernatants or biomass from end point samples of the various cultivations.

Table 4: Summarized cultivation and extraction methods for dodecane to 1,12-dodecanediol conversion by use of the different created mutants of *P. polymyxa* DSM 365.

Method	Strain variants	Cultivation Step 1	Cultivation Step 2	Cell disruption	Extraction
1	*P. polymyxa* DSM 365 pHEiP_*alkBLGST* *P. polymyxa* DSM 365 pHEiP_*alkB1*cluster+*alkL*	25 mL culture with MOPPA medium in 300 mL shake flasks. Start OD of 0.025. Incubation at 30 °C and 200 rpm for 48 h. 50 g/L at the start of the cultivation	no	no	Extraction with 25 mL ethyl acetate containing 2 mM decanol as an internal standard. extraction for 15 min at 200 rpm
2	As 1	As 1 but dodecane addition after 24 h	no	no	As 1
3	All strains	As 1 but with start OD of 0.1, 5 mL dodecane and 0.025 % dicyclopropyl keton (DCPK)	no	with and without was tested	As 1 but extraction at 50 °C
4	All strains	As 3 but plus 0.05% TWEEN 80	no	With and without was tested	As 3
5	All strains	As 4 but cultivation only 24 h	Resuspension of cells from step 1 in resting cell buffer (RCB) 1 (1% glucose, 2 mM MgSO4, and 50 mM potassium phosphate buffer pH 7.4). Cultivation at 30 °C and	With and without was tested	As 3

			200 rpm for 48 h		
6	All strains	As 5	As 5 but with RCB 2(0.8 % glycerol, 100 µg/mL $FeSO_4 \cdot 7\ H_2O$, 0.2 M sodium phosphate buffer pH 7)	With and without was tested	As 3

2.2 *Pseudomonas fluorescens*

2.2.1 Assessing the Presence of Alkane Degradation Genes in Candidate Strains Through BLAST analysis

P. fluorescens strains are usually known to grow on alkanes and withstand their toxicity, making them interesting strains for WP4 of the ACTPAC project. To assess if *P. fluorescens* SBW25 encodes for the key *Alk* proteins involved in alkane degradation, a BLAST search using the protein sequences of the *alk* genes of *P. putida* GPo1 as queries, identified AlkB, AlkT, and AlkG homologs in *P. fluorescens* SBW25. Yet, AlkL, and AlkS were not identified. AlkL encodes the outer membrane transporter responsible for alkane uptake into the periplasm, and AlkS, the transcriptional regulator of the *alk* operon (Table 5).

Table 5: BlastP results for the *P. putida* GPO1 proteins for alkane hydroxylation and the proteins of *P. fluorescens* SBW25.

Gene	Query coverage	Sequence Identity
alkB	94 %	39.8 %
alkG	61 %	54.9 %
alkT	82 %	36.6 %
alkL	/	/
alkS	/	/

2.2.2 Assessing Growth on Alkanes of *P. fluorescens* SBW25 on Solid Media

Although *alkL* and *alkS* are absent in *P. fluorescens* SBW25, growth experiments on alkanes were conducted to investigate whether alternative genes might support alkane utilization. For growth analysis on solid media, cells were initially cultured overnight on M9 glucose agar, then transferred to M9 agar plates lacking a carbon source. A filter paper soaked with 500 µL of the respective alkane was placed in the lid of each Petri dish, and the plates were incubated at 30 °C for up to seven days. *Pseudomonas aeruginosa,* a very well-known pathogenic (risk class 2 strain) that efficiently utilizes alkanes*,* served as a positive control. As shown in (Figure 7), *P. fluorescens* exhibited slight growth under these conditions. However, the negative control by using agar plates with no alkane provided, revealed similar growth, suggesting that the strain can utilize the agar itself as a carbon source and finally suggesting the inability of the strain to utilize the alkanes (data not shown). In contrast, *P. aeruginosa* demonstrated substantially greater growth, confirming effective alkane utilization under the same conditions.

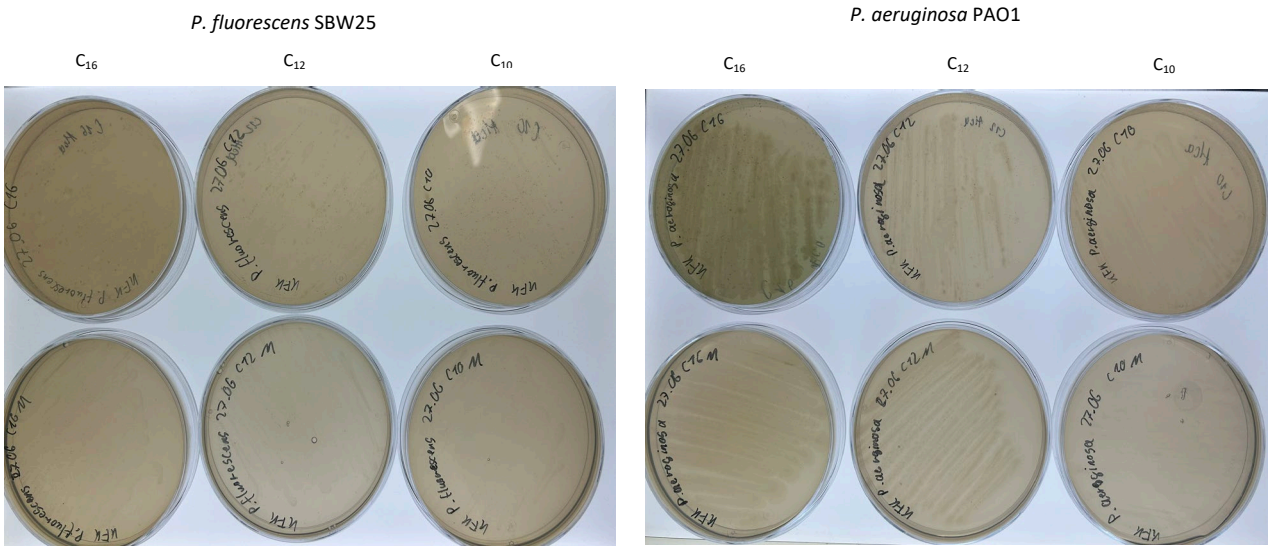

Figure 7. Growth of *P. fluorescens* SBW25 and *P. aeruginosa* PAO1 on M9 agar plates containing no carbon source. 500 µL of alkanes were either applied directly onto plate (top plates) or supplied through gas phase (bottom plates). Cells were grown for 5 days at 30°C. P. fluorescens shows some limited growth which can be attributed to organic contaminants in the used agar, as this growth was also present on plates with no alkanes.

2.2.3 Genetic Engineering of *P. fluorescens* SBW25

To enable the alkane conversion, an alkane inducible expression plasmid was constructed starting from the pWBT plasmid backbone and adding the *P. putida* GPO1 *alk* genes [38]. The T5 lac promoter and lacI of the pWBT plasmid were exchanged with the alkane-degrading genes *alkBLGS* and *T* from *P. putida* GPO1. Gene expression was driven by the native promoter and *alk*S and *alkT* were organized in one operon, whereas *alkBL*, and *G* constituted a second operon, resulting in the plasmid pWBT_*alkBLGST* (Figure 8).

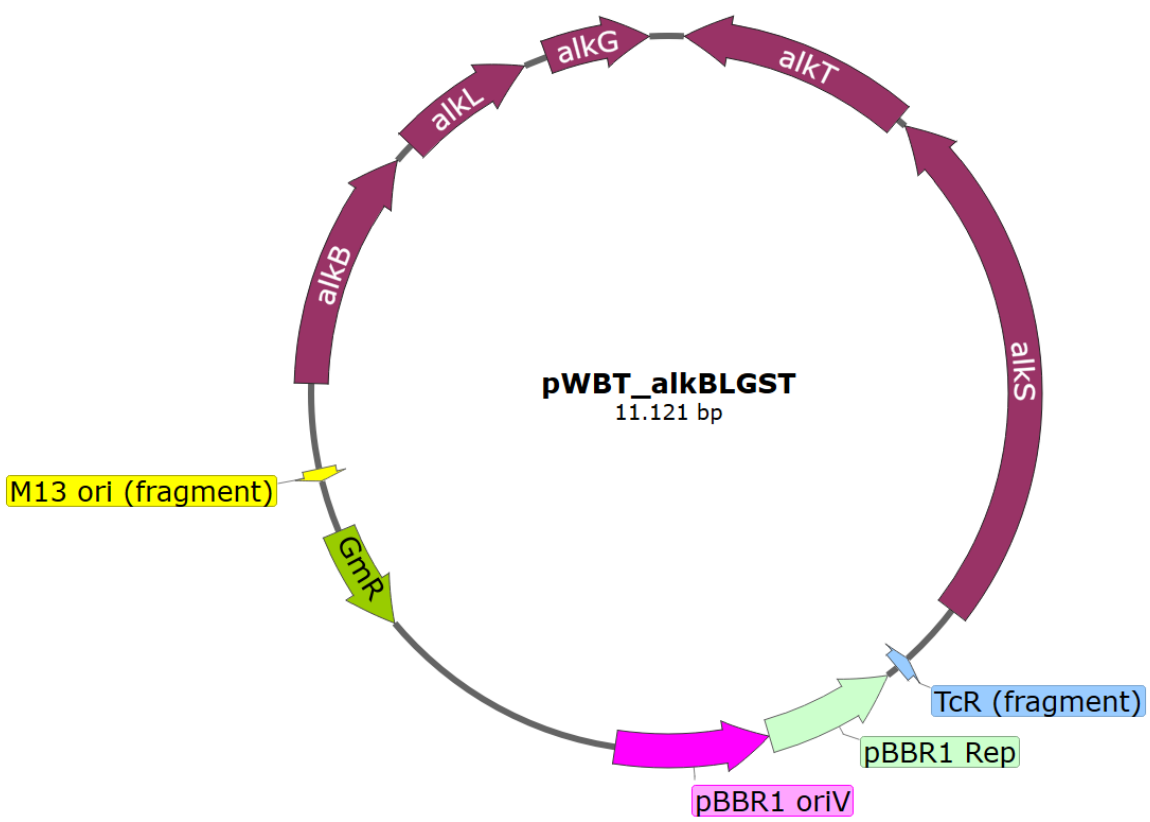

Figure 8. pWBT_Palk_*alkBLGST* plasmid. Plasmid constructed from the pWBT plasmid via the exchange of the T5 lac promoter. The two operons *alkST* and *alkBLG* of *P. putida* GPO1 are arranged under their native promoters.

The plasmid was transferred to *P. fluorescens* SBW25 via triparental mating using *E. coli* S17-1 (donor strain), *E. coli* HB101 carrying the helper plasmid pRK2013, and *P. fluorescens* SBW25 wildtype as the recipient [39]. To assess whether the plasmid conferred the ability to grow on alkanes, the engineered strain was plated on M9 agar with dodecane supplied through the gas phase as described in the previous section. After 4 days of incubation at 30 °C, successful expression of the *alk* genes was indicated by the appearance of colonies (Figure 9). A clear difference is noticeable between the control without dodecane addition and the one with. However, when the strain was cultivated in M9 liquid media with dodecane as the sole carbon source, no growth was observed (data not shown).

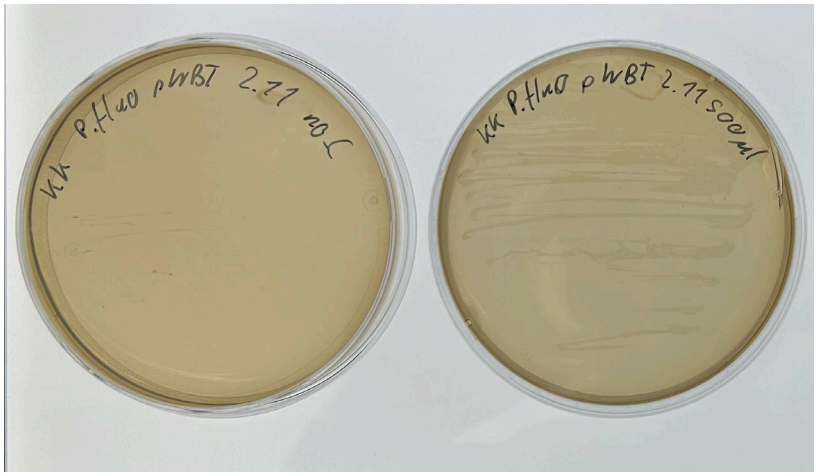

Figure 9. *P. fluorescens* pWBT_Palk_*alkBLGST* on M9 agar plates with only dodecane as carbon source. On the left, the control without dodecane (no C-source), on the right, the strain with supplied dodecane. The strain was incubated for 4 days at 30 °C.

At the same time, a rearrangement of the order of the genes in the plasmid was decided. Previous studies showed that rearranging gene order within an operon can enhance the performance of the whole system [40]. Since the reaction catalysed by AlkG is considered the rate-limiting step, the operon was rearranged from alkBLG to alkGBL, resulting in the construct pWBT_Palk_*alkGBLST*. To also exclude that the expression itself was the main issue, the inducible T5 promoter was used instead of the *alk* native promoters, resulting in plasmid variants pWBT_T5_alkBLGT and pWBT_T5_alkGBTL. Both constructs were designed without the *alkS* gene. These variants were first grown on agar plates, but no clear effect of the gene arrangement was observable (Figure 10). Growth on liquid M9 medium was tested using 2 g/L citrate instead of glucose, since the citrate does not suppress the *alk* promoter. Strains with plasmids containing the T5 promoter were induced with 1 mM IPTG, and strain variants with plasmids containing the native *alk* promoter with 0.05 % DPCK. However, no clear difference between the strains with and without dodecane was observed, indicating that the strains are still not utilizing alkanes for growth (Figure 11).

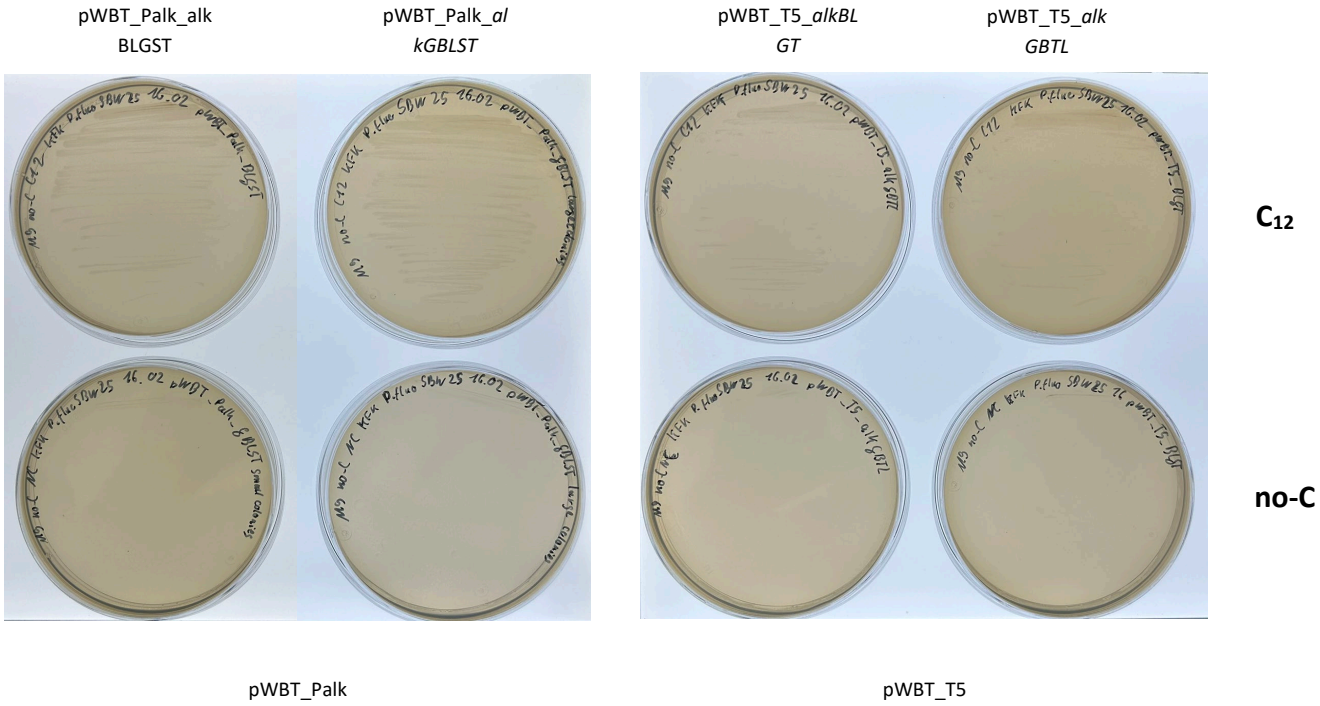

Figure 10. Growth of *P. fluorescens* SBW25 on M9 plates without additional carbon source with either plasmids pWBT_Palk_*alkBLGST*, pWBT_Palk_*alkGBLST*, pWBT_T5_*alkBLGT,* or pWBT_T5_*alkGBTL*. Dodecane was supplied through the gas phase to the upper plates, with the lower plates being the negative control.

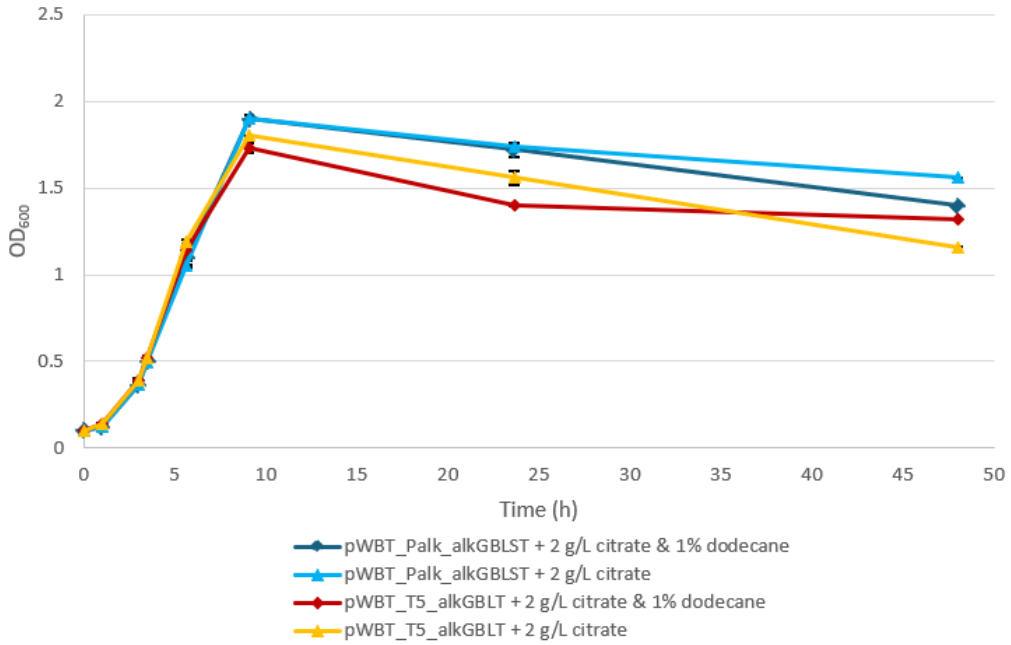

Figure 11: Growth of *P. fluorescens* SBW25 in M9 medium with either pWBT_Palk_*alkGBLST* or pWBT_T5_*alkBLGT*, with or without dodecane as C-source. Cells were grown to OD_{600} of 0.5 before being induced with either 0.05 % DCPK for Palk or 1 mM IPTG for PT5. Cells were grown at 30°C at 120 rpm. Dots indicate the mean, error bars the standard deviation (n = 2)

Due to the system's continued inefficiency and limited responsiveness to modifications, it was suspected that a crucial component might be absent. So, it was decided to increase the cultivation period and additionally to include *alkF*, the second rubredoxin encoded on the OCT plasmid, in the various constructs. While literature typically attributes *alkBGT* to the conversion of alkanes to fatty alcohols, supported by *alkL* and *alkS* for transport and regulation [41, 42], most studies utilizing OCT plasmid-based systems for fatty alcohol production retain the full plasmid, excluding only *alkJ*, which encodes an alcohol dehydrogenase [43, 44]. Although AlkF is considered a non-functional, N-terminally truncated variant of AlkG, its retention in the plasmid might still have served a purpose. Consequently, *alk*F was cloned under control of the *alk* promoter, resulting in plasmid pWBT_Palk_*alkGFBLST*. After transformation, the mutant strain was tested in M9 medium supplemented with 2 g/L citrate with two different pH settings (6.3 and 7) to evaluate whether lower pH affects alkane metabolism. Cultures were inoculated to OD_{600} = 0.1, with 1 % dodecane and 0.05 % DCPK, as an additional inducer, from the start of the inoculation. After three days, 500 µL of dodecane was added to compensate for usage and evaporation (Figure 12).

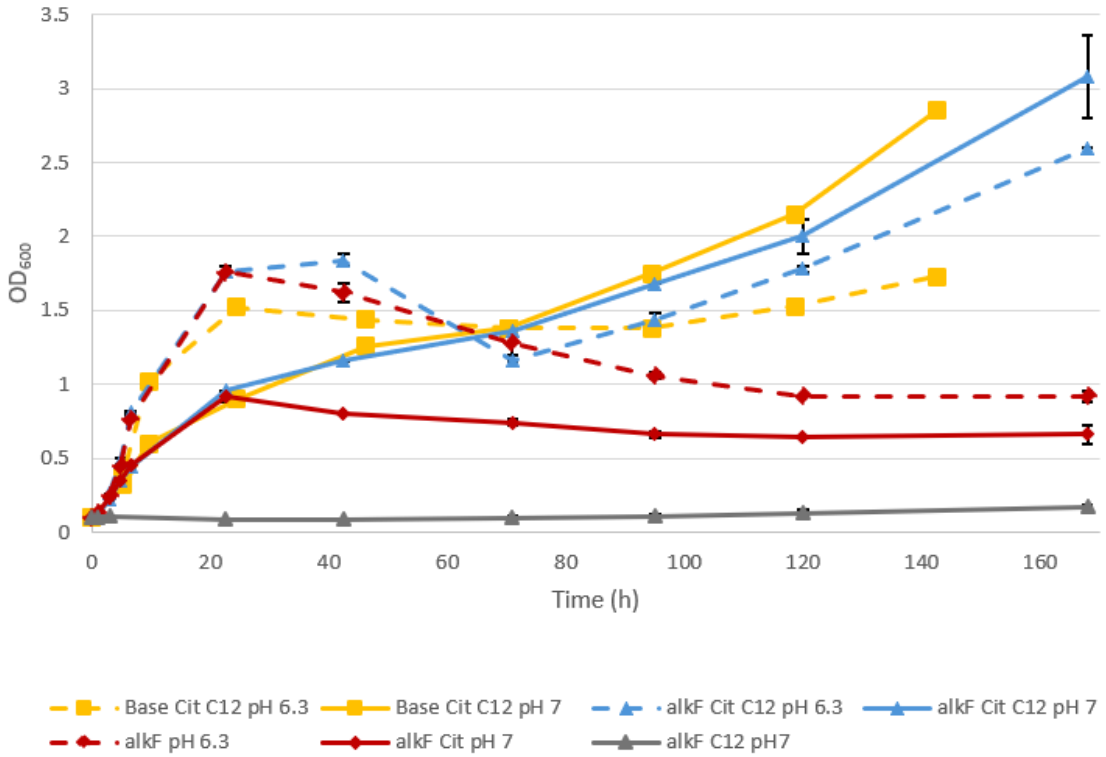

Figure 12. Growth of *P. fluorescens* SBW25 in M9 medium with 2 g/L citrate using different construct variations: base refers to pWBT_Palk_*alkGBLST* without *alkF*. The *alkF* constructs refer to the strain variants with pWBT_Palk_*alkGFBLST* that includes *alkF*. Cells were grown at 30 °C at 120 rpm with 0.05 % of DCPK added from the beginning. Negative controls did not contain any alkanes, while the other cultures contained 1 % dodecane from the beginning on, with additional 1 % dosage after 3 days. Dots indicate the mean, error bars the standard deviation (n = 2)

At pH 7, cultures reached only half the OD_{600} of those at pH 6.3, and cells began metabolizing alkanes, reaching a final OD_{600} of 3. In contrast, pH 6.3 cultures grew efficiently on citrate, followed by a decline in OD_{600} before resuming growth after three to four days. Overall, AlkF does not appear to be strictly necessary for the functionality of the system. However, its expression may impose a slight metabolic burden, particularly at neutral pH. Interestingly, at pH 6.3, AlkF-containing cultures initially dropped

more in OD_{600} but recovered marginally faster than those without, compared to the wildtype *P. fluorescens* SBW25 control strain which grew very similar at pH 6.3 and 7. This indicates that the metabolization of citrate is not inherently worse at pH 7, but that the presence of the plasmid construct causes the pH sensitivity (Figure 13).

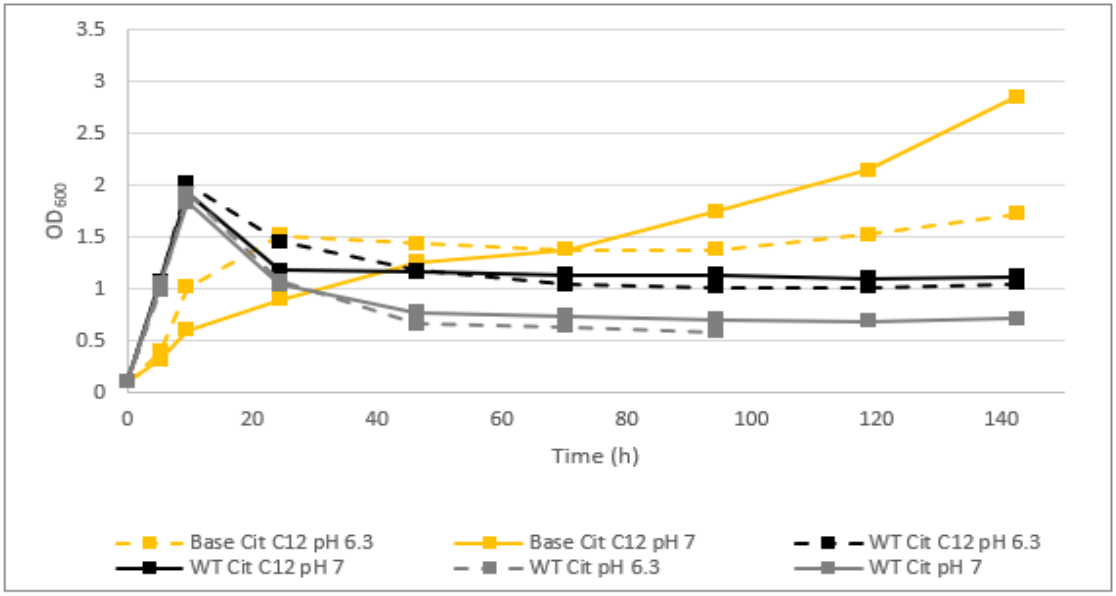

Figure 13. Growth of *P. fluorescens* SBW25 in M9 medium with 2 g/L citrate using different construct variations: base refers to pWBT_Palk_*alkGBLST* without *alkF*. The *alkF* refers to the strain with pWBT_Palk_*alkGFBLST* that includes *alkF*. Cells were grown at 30 °C at 120 rpm with 0.05 % of DCPK added from the beginning on. Negative controls did not contain any alkanes, while the other cultures contained 1 % dodecane from the beginning on with another dosage of 1 % after 3 days. The wildtype without alkanes aggregated quite strongly, causing a stronger decrease in OD_{600}. Squares indicate the mean, error bars the standard deviation (n = 2).

All strain variants which were created for *P. fluorescens* SBW25 are summarized in Table 6.

Table 6: Mutant variants of *P. fluorescens* SBW25 engineered for alkane to α-ω-diol conversion.

Strain	Plasmid	Description
P. fluorescens SBW25 pWBT_*alkBLGST*	pWBT_*alkBLGST*	pWBT with genes for terminal alkane hydroxylation from *P. putida* GPo1
P. fluorescens SBW25 pWBT_*alkGBLST*	pWBT_*alkGBLST*	pWBT with genes for terminal alkane hydroxylation from *P. putida* GPo1, with *alkG* at the starting position of the cluster
P. fluorescens SBW25 pWBT _*alkGFBLST*	pWBT_*alkGFBLST*	pWBT with genes for terminal alkane hydroxylation from *P. putida* GPo1, with *alkG* at the starting position of the cluster and *alkF* included

P. fluorescens SBW25 pWBT_T5_*alkBLGT*	pWBT_T5_*alkBLGT*	pWBT with genes for terminal alkane hydroxylation from *P. putida* GPo1 under control of the T5 promoter instead of *Palk*
P. fluorescens SBW25 pWBT_T5_*alkGBTL*	pWBT_T5_*alkGBTL*	pWBT with genes for terminal alkane hydroxylation from *P. putida* GPo1, with *alkG* at the starting position of the cluster under control of the T5 promoter instead of *Palk*

2.3 *Pseudomonas putida* KT2440

2.3.1 Plasmid Design and Strain Engineering for Alkane to α-ω-Diol Conversion in *P. putida* KT2440

Due to the proven functionality by the former experiments in *P. fluorescens*, the plasmids pWBT_*alkBLGST*, pWBT_*alkGBLST* and pWBT_*alkGFBLST* were chosen for the first engineering attempts in *P. putida* KT2440. Additionally, the plasmid pSEVA258_*alkB*FLG*ST* (Figure 14) was designed and constructed. This plasmid contains the genes encoding for enzymes enabling alkane hydroxylation in *P. putida* GPo1, but with modified versions of *alkB* and *alkG*. For those genes the attachment sites for the Crc/Hfq protein complex were deleted from the 5' untranslated region (UTR) to decrease the effects of the carbon catabolite repression machinery in the host. Additionally, the natural promoter of the cluster, including its transcriptional activator AlkS was exchanged with the Pm promoter together with the XylS regulator.

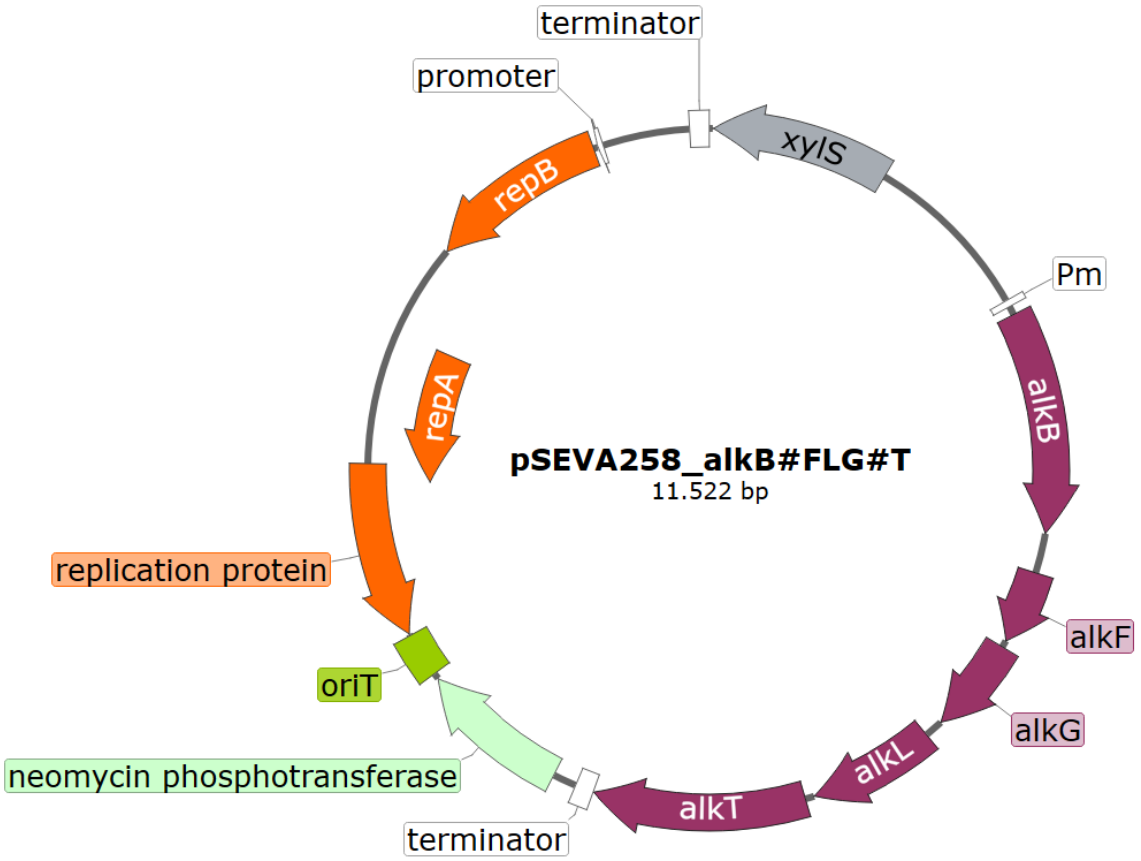

Figure 14: Schematic structure of pSEVA_*alkB*FLG*T* including a neomycin resistance gene for selection and *XylS* for induced activation of the Pm promoter, *alkB encoding a modified version of the alkane hydroxylase from the OCT plasmid, modified *alkG* and *alkT* encoding the rubredoxin and rubredoxin reductase from the OCT plasmid, *alkL* encoding the alkane transporter from the OCT plasmid.**

All plasmids from this chapter were cloned successfully and transferred to *P. putida* KT2440. Accordingly, all the designed strain variants are listed in Table 7.

Table 7: Mutant *P. putida* KT2440 strains constructed for alkane to α-ω-diol conversion.

Strain	Plasmid	Description
P. putida KT2440 pWBT_*alkBLGST*	pWBT_*alkBLGST*	pWBT with genes for terminal alkane hydroxylation from *P. putida* GPo1
P. putida KT2440 pWBT_*alkGBLST*	pWBT_*alkGBLST*	pWBT with genes for terminal alkane hydroxylation from *P. putida* GPo1, with *alkG* at the starting position of the cluster
P. putida KT2440 pHEiP_*alkGFBLST*	pWBT _*alkGFBLST*	pWBT with genes for terminal alkane hydroxylation from *P. putida* GPo1, with *alkG* at the starting position of the cluster and *alkF* included

P. putida KT2440 pSEVA258_*alkB*FLG*T*	pSEVA258_*alkB*FLG*T*	Carries all genes for terminal alkane hydroxylation from *P. putida* GPo1, with modified *alkB* and *alkG* (attachment sites for Crc/Hfq complex deleted) and *alkF* included

2.3.2 Test Cultivations Using Mutant *P. putida* KT2440 Strains for Alkane Oxidation

A first test cultivation was performed with *P. putida* KT2440 pWBT_*alkGFBLST*, *P. putida* KT2440 pSEVA258_*alkB*FLG*T* and the wild type strain used as a negative control. Precultures of 25 mL liquid culture *P. putida* KT2440 pWBT_*alkGFBLST* and *P. putida* KT2440 pSEVA258_*alkB*FLG*T* were cultivated in M9 medium with the appropriate antibiotic overnight at 30 °C and 250 rpm. The next day, new 25 mL cultures were started from the precultures using M9 media with the appropriate antibiotic and a starting OD_{600} of 0.625. Additional 6.25 µL of DCPK was given to the *P. putida* KT2440 pWBT_*alkGFBLST* cultures as an inducer for *alk* gene expression. To *P. putida* KT2440 365 pSEVA258_*alkB*FLG*T* 50 µL of a 100 mM stock solution of 3-methylbenzoate was added as an inducer for *alk* gene expression. Both inducers were added to the wild type, to serve as a control. Cultures were incubated for 5 h at 30 °C and 200 rpm. After 5 h, all cultures were resuspended to an OD of 3 in resting cell buffer (1 % glucose, 2 mM $MgSO_4$, potassium phosphate buffer at pH 7). Next, 990 µL of the suspensions were filled into three 40 mL reaction tubes with lids containing rubber O-rings each (n=3). Finally, 10 µL hexane was added to each reaction tube. The conversions were run for 48 h at 30 °C and 250 rpm. Extraction was performed with ethyl acetate containing 2 mM decanol as an internal standard for 15 min at 50 °C. An obtained chromatogram is shown on the example of pWBT n1 in Figure 15.

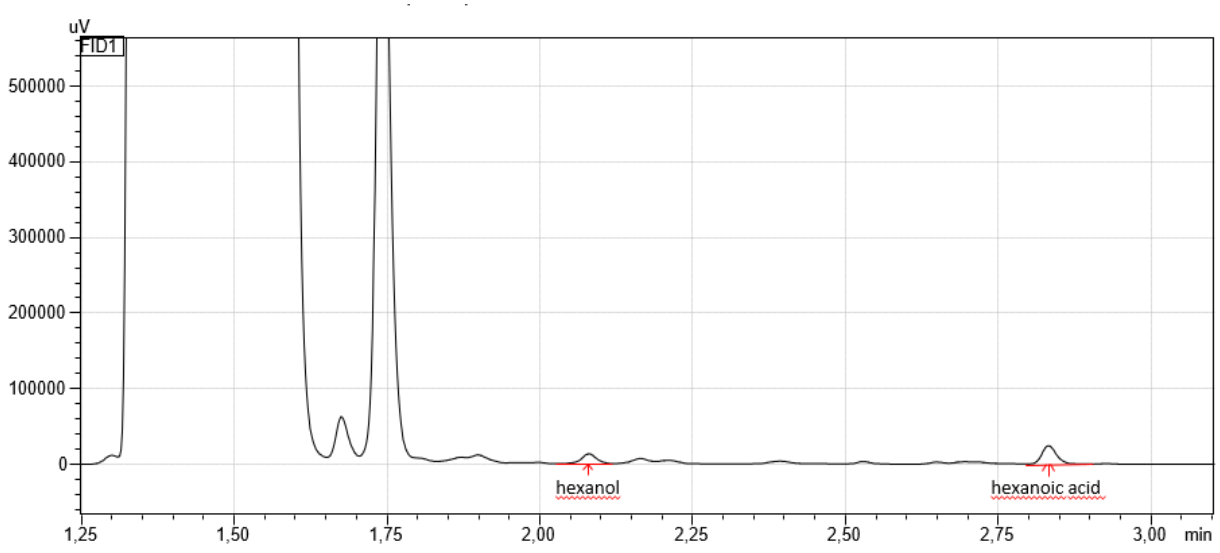

Figure 15: Chromatogram from the first replica (n1) of from the conversion with *P. putida* KT2440 pWBT *alkGFBLTS.*

For both tested mutant strains, oxidation products of hexane were obtained, while no oxidation products were observed for the wild type. For *P. putida* KT2440 pWBT_*alkGFBLST* 0.77 mM of hexanol and 0.76 mM of hexanoic acid were obtained (Figure 16). For *P. putida* KT2440 pSEVA258_*alkB*FLG*T* slightly lower concentrations of 0.70 mM hexanol and 0.67 mM of hexanoic acid were measured (Figure 16). This indicates that the genes on these constructed plasmids are functionally expressed and that AlkB can perform the desired hydroxylation. Interestingly, the pSEVA containing mutant led to lower product concentrations compared to the pWBT mutant, even though it carries the optimised versions of the *alkB* and *alkG* genes. This might be attributed to the use of the different promoters. By that, the strength of the different promoters and their effect on alkane conversion will be addressed in future experiments.

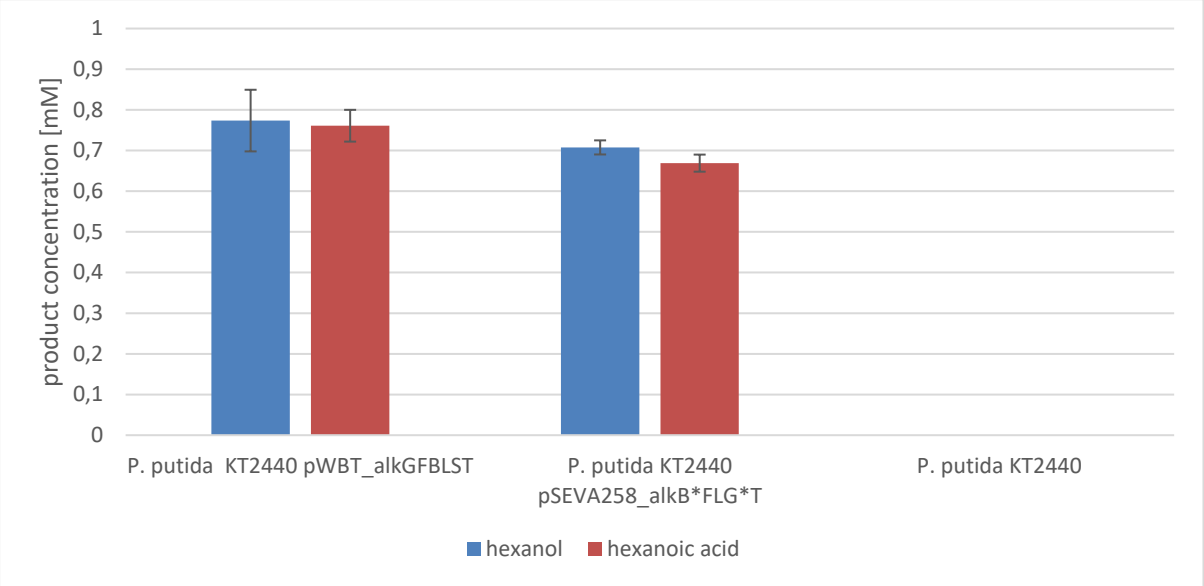

Figure 16: Obtained titers of hexanol and hexanoic acid from the conversions using *P. putida* KT2440 pWBT_*alkGFBLST* and *P. putida* KT2400 pSEVA258_*alkB*FLG*T*. Columns indicate the mean, error bars the standard deviation (n =3).

Overall, these results confirmed that these two constructs are functional, and provide a first basis for alkane hydroxylation using whole cell biocatalysts. Based on this, the next steps will include the modification of these constructs towards long-chain alkane conversion by introducing the *R. erythropolis* PR4 *alkB1* and *alkB2* genes. Further engineering will address increased conversion rates, minimised overoxidation on one end of the alkane to push the system towards diterminal hydroxylation.

2.4 In Silico Analysis of AlkB Reaction System

2.4.1 Docking Studies of AlkB

Due to the missing information on how the substrates behave during uptake in the outer membrane of Gram-negative bacteria, a modelling approach was performed for the AlkB protein. AutoDock Vina was used to model how AlkB interacts with two alcohols: dodecanol and hexadecanol. For dodecanol, the enzyme preferred to bind the molecule with the alcohol group facing the active site and the ω-

carbon pointing outward. For hexadecanol, the binding was varied, but most stable positions still usually had the alcohol pointing inward. This suggests that AlkB may naturally prefer having molecules in which the alcohol group enters the active site first. This preference might make it harder for the ω-carbon to reach the active site. It must be highlighted that AutoDock Vina does not account for the process of the substrate moving into the binding pocket, but immediately starts with a conformation where the construct is positioned within it and subsequently optimizes it to achieve the lowest energy coordinates. It therefore represents a global optimum and does not account for any unfavourable intermediate conformations that would need to be overcome to achieve the ideal substrate position. The resulting conformation is thus not necessarily preferred. This positioning of the alcohol could, however, explain AlkB's tendency to overoxidize its products.

2.4.1 Substrate Behaviour in Membrane

During molecular dynamics (MD) simulations aimed at studying AlkB's substrate channel, it was found that dodecane exits the enzyme through a side opening between transmembrane helices 1 and 2, located in the middle of the membranes (Figure 17). This means that any molecule AlkB acts on must first enter the membrane. Based on this, we speculated that some molecules, like-long chain alcohols might not enter the membrane easily due to their amphipathic nature.

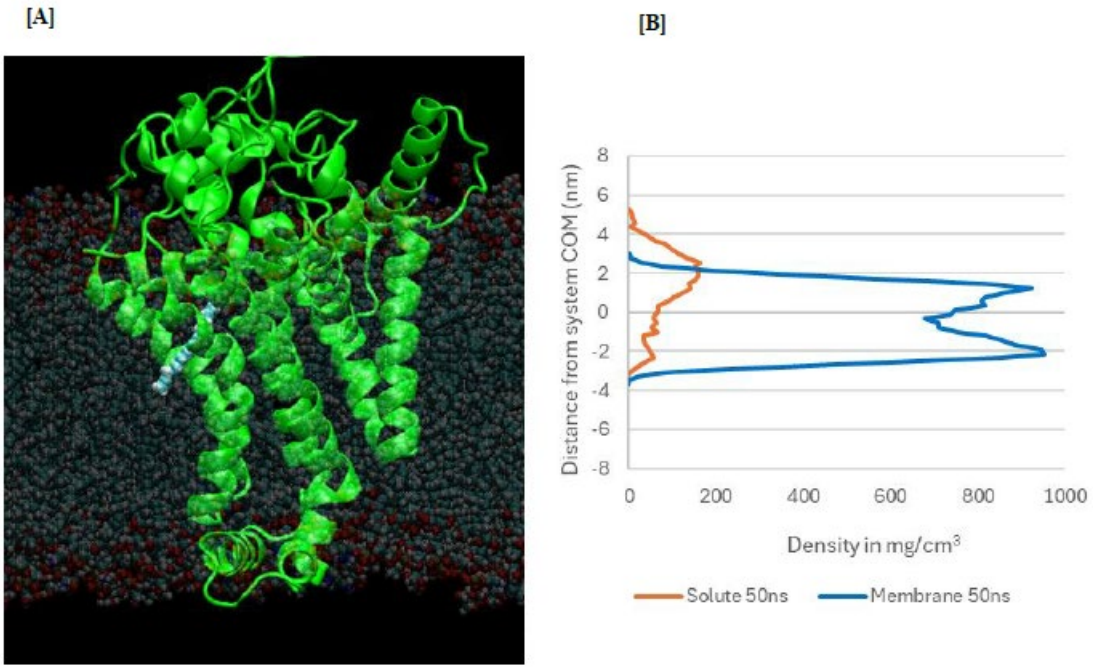

Figure 17. [A] Snapshot of a molecular dynamics simulation run shows dodecane leaving the P. fluorescens SBW25 AlkB substrate channel into the membrane. [B] Density plot of the membrane and AlkB after a 50 ns run. The membrane shows its highest density around the head groups, with the density decreasing towards the mobile lipid tails.

To test this, all-atom MD simulations were run in GROMACS, using a realistic membrane built with CHARMM-GUI. Five molecules of different compounds were randomly placed into the membrane, replacing lipids where necessary. After 200 ns of simulation, the z-height position of the terminal heavy atoms in each molecule was tracked and normalized against the dynamic center of mass (COM) of the membrane. This normalization was necessary because of the membrane's compressibility. This

compressibility leads to fluctuations of the x and y dimensions of the simulation box, and as the water on both sides of the membrane is practically incompressible, it gets pushed out and pulled in continuously, changing the z-axis length and thereby z-height of the membrane. In the simulation shown as an example in Figure 18, membrane COM fluctuations of around 0.4 nm were observed.

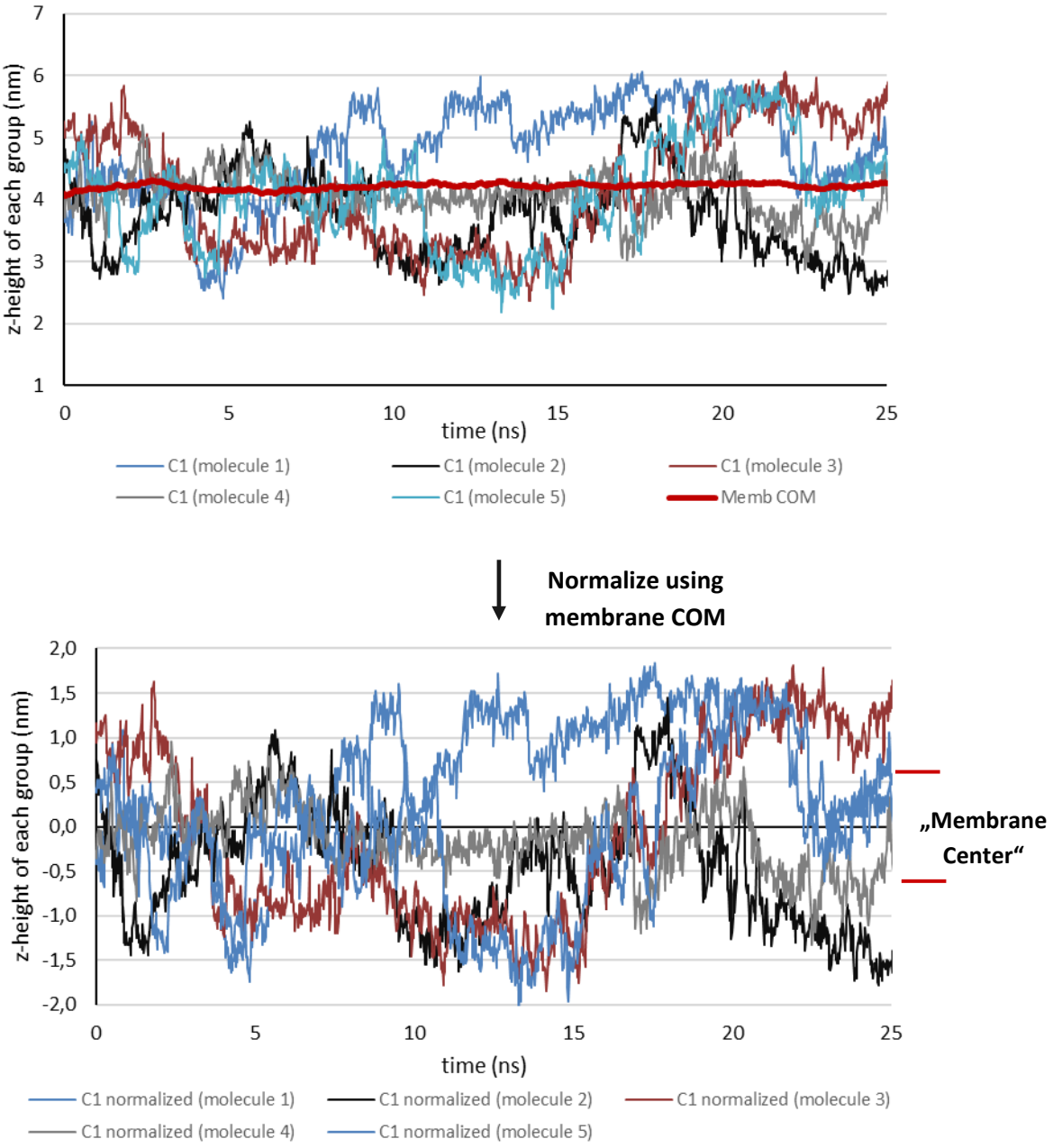

Figure 18. Example of the methodology for tracking molecule movement in the membrane along the z axis shown for the C1 atoms of five dodecane over 25 ns. Index groups of the terminal heavy atoms were created and tracked over the run as well as the membrane COM. The positions were then normalized against the membrane center of mass and the fraction of time spend within 0.6 nm determined.

2.4.2 Alkane Movement in Membrane

Alkanes move freely within the membrane and frequently align horizontally relative to the membrane, particularly at shorter lengths, positioning themselves in the centre of the bilayer, which would make them highly available to AlkB (Figure 19).

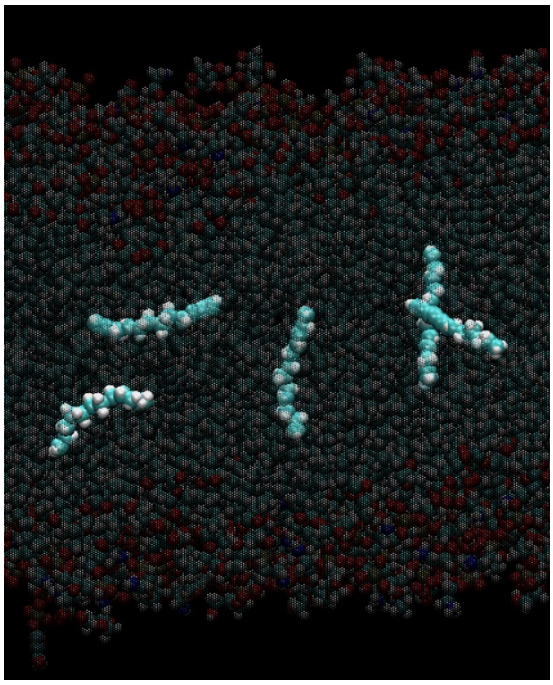

Figure 19. Exemplary positions of dodecane during a simulation run. Shown in opaque are the dodecane molecules with the membrane lipids displayed see-through and the water molecules hidden.

0.6 nm in each direction from the membrane COM was defined as the "membrane middle" for all analysis. This was based on the observation that, from that distance towards the membrane COM, the concentration of alkanes started increasing fast (Figure 20).

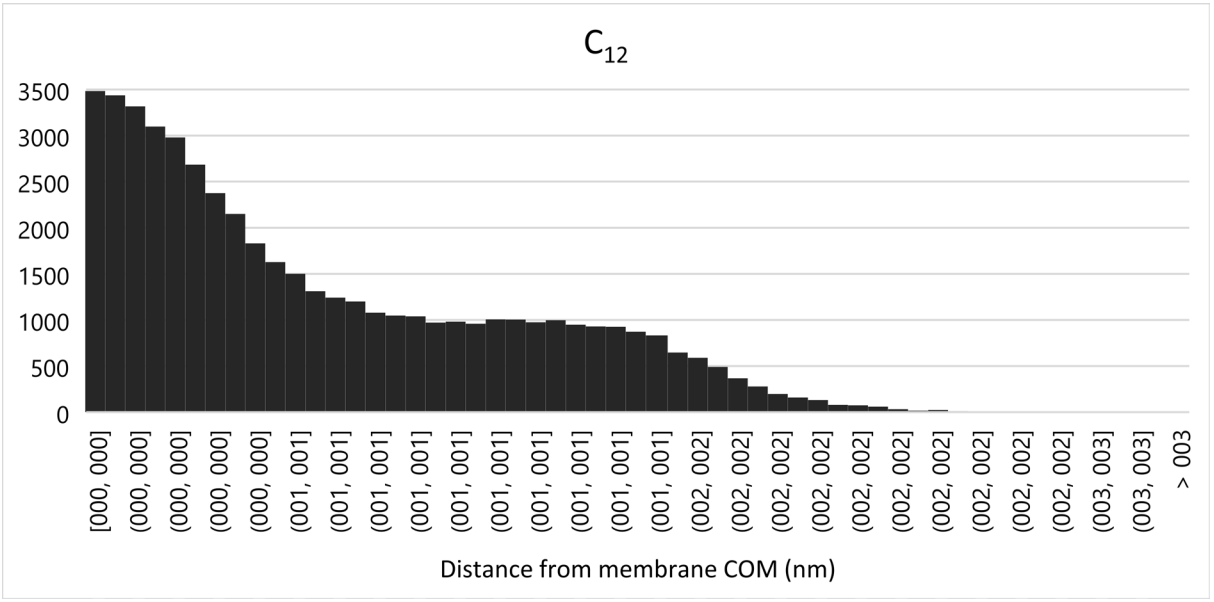

Figure 20. Histogram of the distance of the terminal carbon atoms of dodecane to the membrane COM over a 200 ns run. Only one terminal atom per molecule was tracked for this graph.

2.4.3 Alcohols and Esters Movement in Membrane

After analysing how the alkanes behave in the membrane, it was tested how the alcohols behave. These alcohols behaved noticeably differently from the alkanes. Throughout most of the simulation, the fatty alcohols remained in a vertical orientation, with their hydroxyl (–OH) groups positioned near the charged head groups of the membrane lipids (Figure 21).

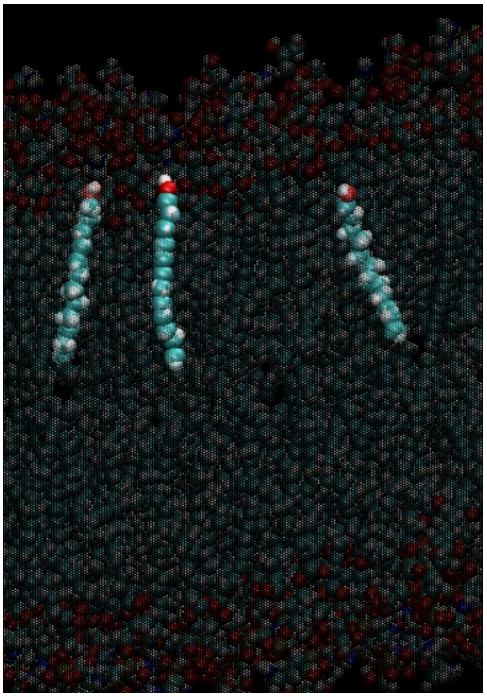

Figure 21. Exemplary positions of dodecanol during a run. Shown in opaque are the dodecane molecules with the membrane lipids displayed see-through and the water molecules hidden.

Simulations revealed that fatty alcohols like hexanol and decanol enter the central region of the membrane only rarely—about 0.5 % of the time. This frequency drops sharply for longer-chain alcohols like dodecanol (0.1 %) and hexadecanol (0.004 %), which behave more like membrane lipids (Figure 22).

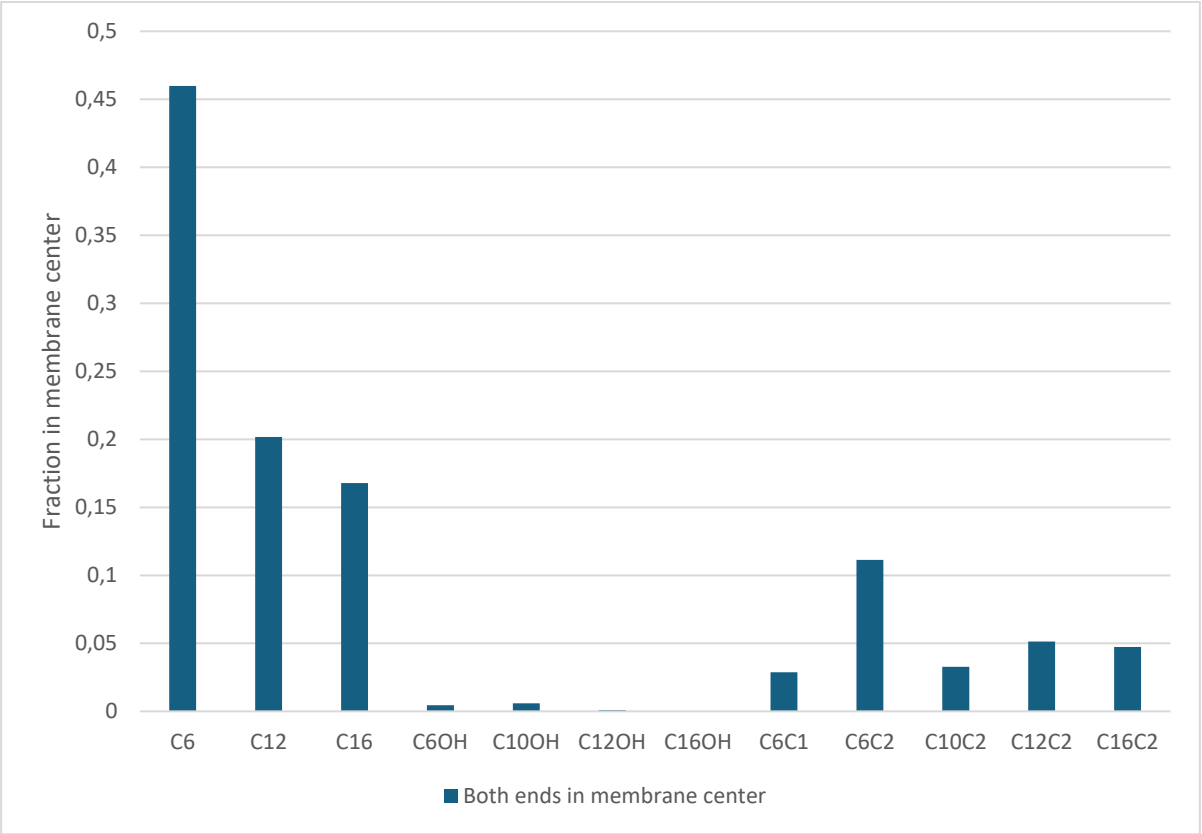

Figure 22. Extrapolated fraction of different compounds with both molecules ends within 0.6 nm of the membrane center. Five molecules of each substrate were inserted into a membrane system, and the simulation ran for 200 ns. Shown from left to right are alkanes, alcohols, and esters, with the chain length of both chains of the ester given. (n = 1).

These results suggest that the limited activity of AlkB is mainly due to how substrates are distributed in the membrane, not just the enzyme's structure. Since long-chain alcohols are poorly soluble in water (e.g., solubility falls below 0.1 µg/L for chains longer than C15), modifying them into esters is currently the best strategy to enable ω-oxidation and diol production, as it improves their membrane behavior and accessibility to the enzymes. Hexanoic acid ethyl ester displays the highest absolute value at 11.1 % in the membrane centre, a 24-fold increase over hexanol, while hexadecanoic acid ethyl ester shows the highest relative improvement compared to the alcohol with 4.7 % in the middle region, a 1,200-fold higher concentration compared to hexadecanol (Figure 22).

3 Conclusions

For *P. polymyxa* DSM 365 five different strains for alkane-to-α,ω-diol conversion were created and tested. However, no detectable alkane hydroxylation was observed under the tested conditions. Since *P. polymyxa* showed no growth limitation in the presence of dodecane, but also no alkane conversion, it is likely that substrate uptake is restricted, preventing both gene induction and substrate supply for the desired bioconversion. To investigate this hypothesis, we plan to assess transcription of our artificial alkane hydroxylation clusters via RT-qPCR.

However, overall, our work demonstrates the functional implementation of alkane conversion systems in *Pseudomonas* sp. Indeed, an inducible AlkB-based alkane conversion system was successfully developed for use in *Pseudomonas* sp. Four different plasmids were cloned by combining either the native alkane promoter from the OCT plasmid or the T5 promoter, and by rearranging gene order within the *alk* operon. The resulting constructs pWBT_Palk_*alkBLGST*, pWBT_Palk_*alkGBLST*, pWBT_*alkGFBLST*, pWBT_T5_*alkBGLT*, and pWBT_T5_*alkGBLT* enabled the strains to grow on solid dodecane M9 medium. Further tests in liquid M9 medium (using citrate as a carbon source) showed delayed but successful growth on alkanes, suggesting the system becomes functional over extended cultivation in *P. fluorescens* SBW25. Additionally, pH was identified as a factor influencing system performance. The constructs pWBT_*alkBLGST*, pWBT_*alkGBLST* and pWBT_*alkGFBLST* were also transferred to *P. putida* KT2440 as well as the newly designed plasmid pSEVA258_*alkB*FLG*T*. In cultivations, the strain *P. putida* KT2440 pWBT_*alkGFBLST* converted 76 mM (1 %) hexane in 0.77 mM of hexanol and 0.761 mM of hexanoic acid, and for *P. putida* KT2440 pSEVA258_*alkB*FLG*T* converted 0.70 mM hexanol and 0.67 mM of hexanoic acid. These results confirm that the constructs created are functional in these strains and provide a foundation for whole-cell biocatalytic alkane hydroxylation. Even when the conversion of long-chain alkanes into the desired α,ω-diols has not been successfully realized up to now, we have set the complete basis for adapting and optimizing the functional conversion system towards long-chain alkanes within the next steps. By exchanging the *alkB* genes from *Pseudomonas* sp. with the *alkB1* and *alkB2* genes of *R. erythropolis* PR4, is highly promising to realize long-chain alkane conversion with simple adaptations. Further gene deletions such as alcohol and aldehyde dehydrogenases encoding ones will be applied to try to reduce or circumvent the overoxidation.

Finally, docking simulations were performed and showed that AlkB consistently orients the alcohol group towards the active site, which may explain its preference for terminal oxidation and limited ability to perform ω-oxidation. MD simulations also revealed that fatty alcohols, unlike alkanes, remain near the membrane surface due to their amphipathic nature, limiting their access to AlkB. Substrate distribution in the membrane, rather than enzyme structure, appears to restrict activity. From this study, it was elucidated that converting fatty alcohols into esters could improve their membrane dynamics and enable ω-oxidation and diol production, overcoming limitations in solubility and enzyme accessibility.

With the successful implementation of the alkane conversion system, our next aim is to investigate the strain's capability for efficient diol production by deleting alcohol and aldehyde dehydrogenases while adapting the system for long-chain alkanes. For that, *R. erythropolis* PR4 *alkB1* and *alkB2* will be introduced in the existing strains for improved conversion rates, reducing overoxidation at one alkyl

end, and promoting diterminal hydroxylation. Additionally, the conversion of fatty alcohols into esters might be very promising approach to highly improve the production rate of diols and would validate the in-silico analysis. In sum, the final goal of long-chain alkane-to-α,ω-diol conversion was not completely reached, but all foundations were set for promising realization by follow up steps. In addition, the modelling approach identified a putative bottleneck for alkane-to-α,ω-diol conversion for the first time and suggests a very promising solution by the intermediate step of esterification, which might massively boost the conversion rates. By that, D4.2 and WP4 are completed, but M5 is not completely reached. When the following experiments in WP5 will show that the hypothesis of limited long-chain alkane solubility/availability for AlkB and the bacterial membrane, as suggested via the dynamic modelling approach, will come true, the suitability of bacterial long-chain alkane to diol conversion might be questioned for the ACTPAC project.

4 References

[1] C. Lu, N. Leitner, R. H. Wijffels, V. A. P. Martins Dos Santos, and R. A. Weusthuis, “Microbial production of medium-chain-length α, ω-diols via two-stage process under mild conditions,” *Bioresource technology*, vol. 352, p. 127111, 2022, doi: 10.1016/j.biortech.2022.127111.

[2] C. Lu, C. Batianis, E. O. Akwafo, R. H. Wijffels, V. A. P. Martins Dos Santos, and R. A. Weusthuis, “When metabolic prowess is too much of a good thing: how carbon catabolite repression and metabolic versatility impede production of esterified α,ω-diols in Pseudomonas putida KT2440,” *Biotechnol Biofuels*, vol. 14, no. 1, p. 218, 2021, doi: 10.1186/s13068-021-02066-x.

[3] C. Grant, J. M. Woodley, and F. Baganz, “Whole-cell bio-oxidation of n-dodecane using the alkane hydroxylase system of P. putida GPo1 expressed in E. coli,” *Enzyme and Microbial Technology*, vol. 48, 6-7, pp. 480–486, 2011, doi: 10.1016/j.enzmictec.2011.01.008.

[4] Y. M. van Nuland, F. A. de Vogel, E. L. Scott, G. Eggink, and R. A. Weusthuis, “Biocatalytic, one-pot diterminal oxidation and esterification of n-alkanes for production of α,ω-diol and α,ω-dicarboxylic acid esters,” *Metabolic engineering*, vol. 44, pp. 134–142, 2017, doi: 10.1016/j.ymben.2017.10.005.

[5] H. A. Park and K.-Y. Choi, “α, ω-Oxyfunctionalization of C12 alkanes via whole-cell biocatalysis of CYP153A from Marinobacter aquaeolei and a new CYP from Nocardia farcinica IFM10152,” *Biochemical Engineering Journal*, vol. 156, p. 107524, 2020, doi: 10.1016/j.bej.2020.107524.

[6] T. Fujii, T. Narikawa, F. Sumisa, A. Arisawa, K. Takeda, and J. Kato, “Production of alpha, omega-alkanediols using Escherichia coli expressing a cytochrome P450 from Acinetobacter sp. OC4,” *Bioscience, biotechnology, and biochemistry*, vol. 70, no. 6, pp. 1379–1385, 2006, doi: 10.1271/bbb.50656.

[7] N. J. P. Wierckx, H. Ballerstedt, J. A. M. de Bont, and J. Wery, “Engineering of solvent-tolerant Pseudomonas putida S12 for bioproduction of phenol from glucose,” *Applied and environmental microbiology*, vol. 71, no. 12, pp. 8221–8227, 2005, doi: 10.1128/AEM.71.12.8221-8227.2005.

[8] T. Häßler, D. Schieder, R. Pfaller, M. Faulstich, and V. Sieber, “Enhanced fed-batch fermentation of 2,3-butanediol by Paenibacillus polymyxa DSM 365,” *Bioresource technology*, vol. 124, pp. 237–244, 2012, doi: 10.1016/j.biortech.2012.08.047.

[9] G. Ravagnan *et al.,* “Genome reduction in Paenibacillus polymyxa DSM 365 for chassis development,” *Frontiers in bioengineering and biotechnology*, vol. 12, p. 1378873, 2024, doi: 10.3389/fbioe.2024.1378873.

[10] K. Nomura and N. W. Binti Awang, “Synthesis of Bio-Based Aliphatic Polyesters from Plant Oils by Efficient Molecular Catalysis: A Selected Survey from Recent Reports,” *ACS Sustainable Chem. Eng.*, vol. 9, no. 16, pp. 5486–5505, 2021, doi: 10.1021/acssuschemeng.1c00493.

[11] D. R. C. Huybrechts, L. de Bruycker, and P. A. Jacobs, “Oxyfunctionalization of alkanes with hydrogen peroxide on titanium silicalite,” *Nature*, vol. 345, no. 6272, pp. 240–242, 1990, doi: 10.1038/345240a0.

[12] M. Alexander, *Biodegradation and bioremediation,* 2nd ed. San Diego, Calif., Academic Press: Gulf Professional Publishing, 1999.

[13] J. B. van Beilen and E. G. Funhoff, “Alkane hydroxylases involved in microbial alkane degradation,” *Appl Microbiol Biotechnol*, vol. 74, no. 1, pp. 13–21, 2007, doi: 10.1007/s00253-006-0748-0.

[14] S. N. Singh, B. Kumari, and S. Mishra, “Microbial Degradation of Alkanes,” *Microbial Degradation of Xenobiotics*, pp. 439–469, 2012, doi: 10.1007/978-3-642-23789-8_17.

[15] J. B. van Beilen, S. Panke, S. Lucchini, A. G. Franchini, M. Röthlisberger, and B. Witholt, “Analysis of Pseudomonas putida alkane-degradation gene clusters and flanking insertion sequences: evolution and regulation of the alk genes,” *Microbiology (Reading, England)*, vol. 147, Pt 6, pp. 1621–1630, 2001, doi: 10.1099/00221287-147-6-1621.

[16] A. Bosetti, J. B. van Beilen, H. Preusting, R. G. Lageveen, and B. Witholt, “Production of primary aliphatic alcohols with a recombinant Pseudomonas strain, encoding the alkane hydroxylase enzyme system,” *Enzyme and Microbial Technology*, vol. 14, no. 9, pp. 702–708, 1992, doi: 10.1016/0141-0229(92)90109-2.

[17] C. Lu, R. H. Wijffels, V. A. P. Martins Dos Santos, and R. A. Weusthuis, “Pseudomonas putida as a platform for medium-chain length α,ω-diol production: Opportunities and challenges,” *Microbial biotechnology*, vol. 17, no. 3, e14423, 2024, doi: 10.1111/1751-7915.14423.

[18] J. B. van Beilen, J. Kingma, and B. Witholt, “Substrate specificity of the alkane hydroxylase system of Pseudomonas oleovorans GPo1,” *Enzyme and Microbial Technology*, vol. 16, no. 10, pp. 904–911, 1994, doi: 10.1016/0141-0229(94)90066-3.

[19] A. Ratajczak, W. Geissdörfer, and W. Hillen, “Alkane hydroxylase from Acinetobacter sp. strain ADP1 is encoded by alkM and belongs to a new family of bacterial integral-membrane hydrocarbon hydroxylases,” *Applied and environmental microbiology*, vol. 64, no. 4, pp. 1175–1179, 1998, doi: 10.1128/AEM.64.4.1175-1179.1998.

[20] T. H. M. Smits, S. B. Balada, B. Witholt, and J. B. van Beilen, “Functional analysis of alkane hydroxylases from gram-negative and gram-positive bacteria,” *Journal of Bacteriology*, vol. 184, no. 6, pp. 1733–1742, 2002, doi: 10.1128/jb.184.6.1733-1742.2002.

[21] L. G. Whyte, T. H. M. Smits, D. Labbé, B. Witholt, C. W. Greer, and J. B. van Beilen, “Gene cloning and characterization of multiple alkane hydroxylase systems in Rhodococcus strains Q15 and NRRL B-16531,” *Applied and environmental microbiology*, vol. 68, no. 12, pp. 5933–5942, 2002, doi: 10.1128/AEM.68.12.5933-5942.2002.

[22] M. L. Shuler and F. Kargi, *Bioprocess engineering: Basic concepts,* 2nd ed. Upper Saddle River, NJ: Prentice Hall PTR, 2002.

[23] J. V. Pham *et al.,* “A Review of the Microbial Production of Bioactive Natural Products and Biologics,” *Frontiers in microbiology*, vol. 10, p. 1404, 2019, doi: 10.3389/fmicb.2019.01404.

[24] A. K. Pandey, M. J. Barbetti, and J. R. Lamichhane, “Paenibacillus polymyxa,” *Trends in Microbiology*, vol. 31, no. 6, pp. 657–659, 2023, doi: 10.1016/j.tim.2022.11.010.

[25] P. Calero, S. I. Jensen, K. Bojanovič, R. M. Lennen, A. Koza, and A. T. Nielsen, “Genome-wide identification of tolerance mechanisms toward p-coumaric acid in Pseudomonas putida,” *Biotechnology and bioengineering*, vol. 115, no. 3, pp. 762–774, 2018, doi: 10.1002/bit.26495.

[26] P. I. Nikel and V. de Lorenzo, "*Pseudomonas putida* as a functional chassis for industrial biocatalysis: From native biochemistry to trans-metabolism," *Metabolic engineering*, vol. 50, pp. 142–155, 2018, doi: 10.1016/j.ymben.2018.05.005.

[27] THE EUROPEAN PARLIAMENT AND THE COUNCIL OF THE EUROPEAN UNION, "Directive 2000/54/EC of the European Parliament and of the Council," 2020.

[28] L. Lo Piccolo, C. de Pasquale, R. Fodale, A. M. Puglia, and P. Quatrini, "Involvement of an alkane hydroxylase system of Gordonia sp. strain SoCg in degradation of solid n-alkanes," *Applied and environmental microbiology*, vol. 77, no. 4, pp. 1204–1213, 2011, doi: 10.1128/AEM.02180-10.

[29] H.-P. Kleber, R. Claus, and O. Asperger, "Enzymologie der n-alkanoxidation bei acinetobacter," *Acta Biotechnologica*, vol. 3, no. 3, pp. 251–260, 1983, doi: 10.1002/abio.370030309.

[30] T. H. Smits, M. Röthlisberger, B. Witholt, and J. B. van Beilen, "Molecular screening for alkane hydroxylase genes in Gram-negative and Gram-positive strains," *Environmental microbiology*, vol. 1, no. 4, pp. 307–317, 1999, doi: 10.1046/j.1462-2920.1999.00037.x.

[31] A. Tani, T. Ishige, Y. Sakai, and N. Kato, "Gene structures and regulation of the alkane hydroxylase complex in Acinetobacter sp. strain M-1," *Journal of Bacteriology*, vol. 183, no. 5, pp. 1819–1823, 2001, doi: 10.1128/jb.183.5.1819-1823.2001.

[32] J. B. van Beilen *et al.,* "Characterization of two alkane hydroxylase genes from the marine hydrocarbonoclastic bacterium Alcanivorax borkumensis," *Environmental microbiology*, vol. 6, no. 3, pp. 264–273, 2004, doi: 10.1111/j.1462-2920.2004.00567.x.

[33] M. M. Marín, T. H. Smits, J. B. van Beilen, and F. Rojo, "The alkane hydroxylase gene of *Burkholderia cepacia* RR10 is under catabolite repression control," *Journal of Bacteriology*, vol. 183, no. 14, pp. 4202–4209, 2001, doi: 10.1128/jb.183.14.4202-4209.2001.

[34] Y. Wang *et al.,* "Functional characterization of two alkane hydroxylases in a versatile Pseudomonas aeruginosa strain NY3," (in En;en), *Ann Microbiol*, vol. 67, no. 7, pp. 459–468, 2017, doi: 10.1007/s13213-017-1271-5.

[35] K. Laczi *et al.,* "Metabolic responses of Rhodococcus erythropolis PR4 grown on diesel oil and various hydrocarbons," *Appl Microbiol Biotechnol*, vol. 99, no. 22, pp. 9745–9759, 2015, doi: 10.1007/s00253-015-6936-z.

[36] M. Rütering *et al.,* "Tailor-made exopolysaccharides-CRISPR-Cas9 mediated genome editing in *Paenibacillus polymyxa*," *Synthetic biology (Oxford, England)*, vol. 2, no. 1, ysx007, 2017, doi: 10.1093/synbio/ysx007.

[37] M. Sekine *et al.,* "Sequence analysis of three plasmids harboured in Rhodococcus erythropolis strain PR4," *Environmental microbiology*, vol. 8, no. 2, pp. 334–346, 2006, doi: 10.1111/j.1462-2920.2005.00899.x.

[38] E. Krol, C. Klaner, P. Gnau, V. Kaever, L.-O. Essen, and A. Becker, "Cyclic mononucleotide- and Clr-dependent gene regulation in *Sinorhizobium meliloti*," *Microbiology (Reading, England)*, vol. 162, no. 10, pp. 1840–1856, 2016, doi: 10.1099/mic.0.000356.

[39] H. Meng, S. Köbbing, and L. M. Blank, "Establishing a straightforward I-SceI-mediated recombination one-plasmid system for efficient genome editing in *P. putida* KT2440," *Microbial biotechnology*, vol. 17, no. 7, e14531, 2024, doi: 10.1111/1751-7915.14531.

[40] F. Fiorentini, A.-M. Hatzl, S. Schmidt, S. Savino, A. Glieder, and A. Mattevi, “The Extreme Structural Plasticity in the CYP153 Subfamily of P450s Directs Development of Designer Hydroxylases,” *Biochemistry*, vol. 57, no. 48, pp. 6701–6714, 2018, doi: 10.1021/acs.biochem.8b01052.

[41] F. Rojo, *Aerobic Utilization of Hydrocarbons, Oils, and Lipids*. Cham: Springer International Publishing, 2019.

[42] F. Rojo, “Degradation of alkanes by bacteria,” *Environmental microbiology*, vol. 11, no. 10, pp. 2477–2490, 2009, doi: 10.1111/j.1462-2920.2009.01948.x.

[43] Y. M. van Nuland, G. Eggink, and R. A. Weusthuis, “Application of AlkBGT and AlkL from Pseudomonas putida GPo1 for Selective Alkyl Ester ω-Oxyfunctionalization in Escherichia coli,” *Applied and environmental microbiology*, vol. 82, no. 13, pp. 3801–3807, 2016, doi: 10.1128/AEM.00822-16.

[44] G. Eggink, R. G. Lageveen, B. Altenburg, and B. Witholt, “Controlled and functional expression of the Pseudomonas oleovorans alkane utilizing system in Pseudomonas putida and Escherichia coli,” *Journal of Biological Chemistry*, vol. 262, no. 36, pp. 17712–17718, 1987, doi: 10.1016/S0021-9258(18)45437-3.